



## **Final Report**

Project Title: Performances of the Gas Electron Multiplier (GEM)-Based Neutron

Detector using Solid Neutron Converters

By: Dr. Kiadtisak Saenboonruang Kasetsart University

## **Final Report**

**Project Title:** Performances of the Gas Electron Multiplier (GEM)-Based Neutron Detector using Solid Neutron Converters

Researcher Institute

Dr. Kiadtisak Saenboonruang Kasetsart University

Mentor Institute

Prof. Dr. Thiraphat Vilaithong Thailand Center of Excellence in Physics (ThEP)

Prof. Dr. Nilanga K. Liyanage University of Virginia

#### **Abstract**

Project Code: TRG5780292

Project Title: Performances of the Gas Electron Multiplier (GEM)-Based Neutron Detector using Solid

**Neutron Converters** 

Investigator: Dr. Kiadtisak Saenboonruang

E-mail Address: fscikssa@ku.ac.th

**Project Period:** 15 July, 2014 – 14 July 2016

Abstract: The gas electron multiplier (GEM) detector is a gaseous detector that has been utilized for almost 20 years. Since the discovery in 1997 by F. Sauli, the GEM detector has shown excellent properties including high rate capability excellent resolution, low discharge probability, and excellent radiation hardness. These promising properties have led the GEM detector to gain popularity and attention amongst physicists and researchers. In particular, the GEM detector can also be utilized as a neutron detector. Applications of the GEM-based neutron detectors vary from researches in nuclear and particle physics, neutron imaging, and national security. To enable the GEM detector to detect neutrons, an appropriate neutron converter must be added to the detector. Boron-10, which has relatively high neutron cross section compared to other available neutron converters, is a perfect candidate to be used for this purpose. In this research, different thicknesses of pure boron-10 and natural boron films were coated onto a GEM drift cathode such that incoming neutrons could interact via nuclear reactions with boron-10 and produce alpha particles to ionize gas molecules for detection. Results showed that a 1-µm boron-10 film and 2.5-, 3.5-, 4.5-µm natural films coated on the GEM drift cathode were able to detect neutrons emitted from <sup>241</sup>Am/Be, with a 1-µm boron-10 film giving the highest relative efficiency. Efficiencies and gains of the GEM detector increased as the power supply increased, while the efficiencies reached plateau region when the power supply was ~4,200 V. These results indicated the success of using the GEM detector with solid neutron converters to detect neutrons and outcome of the research could be used for future references and researches.

**Keywords:** Gas Electron Multiplier, GEM, neutron, solid neutron converter, boron, radiation

## Final report content:

## 1. Abstract

The gas electron multiplier (GEM) detector is a relatively new gaseous detector that has been utilized for almost 20 years. Since the discovery in 1997 by F. Sauli, the GEM detector has shown excellent properties including high rate capability excellent resolution, low discharge probability, and excellent radiation hardness. These promising properties have led the GEM detector to gain popularity and attention amongst physicists and researchers. In particular, the GEM detector can also be utilized as a neutron detector. Applications of the GEM-based neutron detectors vary from researches in nuclear and particle physics, neutron imaging, and national security. To enable the GEM detector to detect neutrons, an appropriate neutron converter must be added to the detector. Boron-10, which has relatively high neutron cross section compared to other available neutron converters, is a perfect candidate to be used for this purpose. In this research, different thicknesses of pure boron-10 and natural boron films were coated onto a GEM drift cathode such that incoming neutrons could interact via nuclear reactions with boron-10 and produce alpha particles to ionize gas molecules for detection. Results showed that a 1-µm boron-10 film and 2.5-, 3.5-, 4.5-µm natural films coated on the GEM drift cathode were able to detect neutrons emitted from <sup>241</sup>Am/Be, with a 1-µm boron-10 film yielded the highest relative efficiency. Efficiencies and gains of the GEM detector increased as the power supply increased, while the efficiencies reached plateau region when the power supply was ~4,200 V. These results indicated the success of using the GEM detector with solid neutron converters to detect neutrons and outcome of the research could be used for future references and researches.

## 2. Executive summary

The project aims to develop a GEM-based neutron detector using solid neutron converters. To serve the objectives of the project, a 1-μm boron-10 film and 2.5-, 3.5-, 4.5-μm natural films were coated on the GEM drift cathode. Efficiencies and gain of the modified GEM detector were measured by measuring neutron detection count rates and signal amplitudes. Results showed that all configurations of the modified GEM detector were able to detect neutrons emitted from <sup>241</sup>Am/Be, with a 1-μm boron-10 film giving the highest relative efficiency. Efficiencies and gains of the GEM detector increased as the power supply increased, while the efficiencies reached constant or plateau region when the power supply was ~4,200 V.

## 3. Objective

- To characterize performances of different solid neutron converters in the GEM-based neutron detector
- To characterize effects of material thickness used as a solid neutron converter in the GEMbased neutron detector

## 4. Research methodology

## 4.1 Experimental plan and setup

We planned and placed orders on all necessary equipment needed for the experiment. These includes new oscilloscope, electronic components, 99.99% boron-10 and 99.99% natural boron for coating on GEM drift cathodes, and a complete set of 10cm x 10cm GEM prototype kit from GDD group. All equipment have arrived and ready for construction and testing.

## 4.2 Construction and initial functionality tests

After receiving all components and completing preliminary tests such as current leakage tests on all GEM foils, the GEM detector were put together and performed initial tests including gas leakage test, discharge test, and preliminary x-ray detection test using 5.9-keV x-rays from <sup>55</sup>Fe (Fig. 1-4). A gas mixture of Ar/CO<sub>2</sub> (70:30) was flowed through the detector with a constant flow rate of 3.0 L/hr (Fig. 5) during which a high voltage of 4,100 V was supplied to the GEM detector via a voltage divider circuit shown in Fig. 6.



Fig. 1: A micro flow box located inside a cleanroom providing a class-1000 level



Fig. 2: Prototype GEM construction inside the micro flow box



Fig. 3: A closed GEM detector

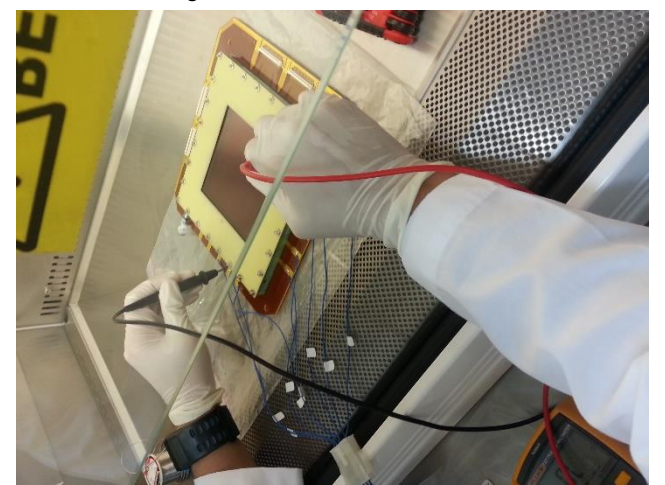


Fig. 4: Electrical check on a closed GEM detector



Fig. 5: A gas assembly for testing.

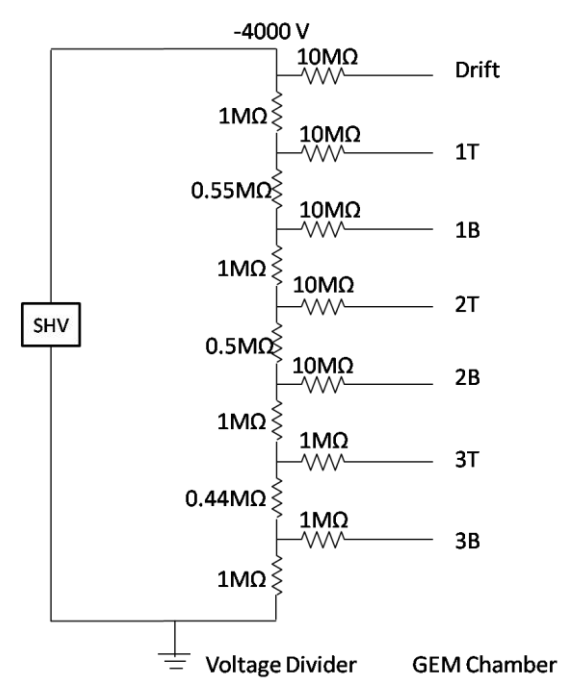


Fig. 6: A voltage divider circuit used to supply high voltages to the GEM detector

The precise gas flow rate was measured by a direct-reading flowmeter (Cole-Parmer Model 3204776) and was adjusted from times to times to ensure steady flow rates throughout the measurement. Since the measurement only recorded counts of detection and average signal amplitudes, the readout strips are combined into one connector and connected to a

preamplifier (Canberra Model 2006), an amplifier (Ortec Model 590A), an oscilloscope, and a counter and timer (Canberra Model 2071A) for data acquisition. The equipment setup for initial tests and neutron tests is shown in Fig. 7.

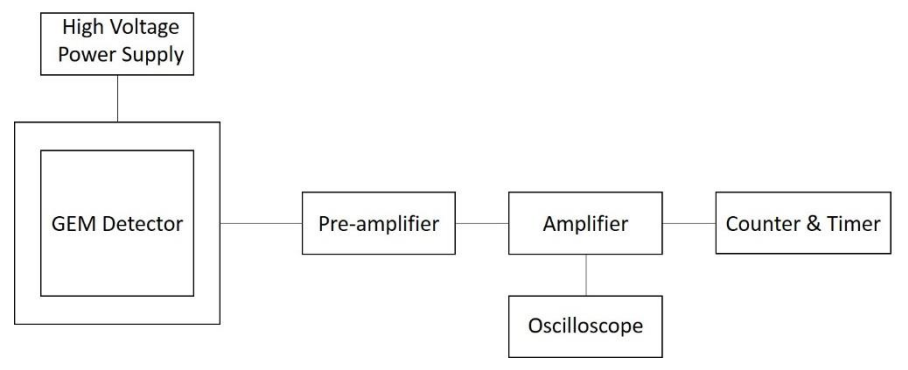


Fig. 7: Schematic setup of the GEM detector during the measurement

After completing all initial tests, 99.9% 10B was coated onto the cathode using Tribo-Kote S-X1 technique performed by Richter Precision, Inc15. However, the manufacturer was only able to coat the cathode with 1-μm thick of <sup>10</sup>B. The picture of a comparison between <sup>10</sup>B-coated cathode and a normal cathode is shown in Fig. 8. In the case of <sup>nat</sup>B, it was coated onto the cathode using an electron beam evaporation technique performed at the National Electronics and Computer Technology Center (NECTEC), Thailand. The coated thicknesses of <sup>nat</sup>B were 2.5, 3.5, and 4.5 μm. Cathodes with <sup>nat</sup>B coating thicker than 4.5 μm have shown some cracks along the film surface and could not be used effectively.

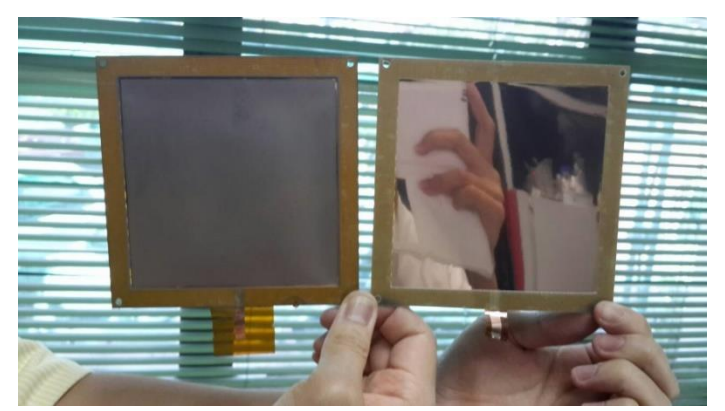


Fig. 8: A comparison between <sup>10</sup>B-coated cathode (left) and a normal cathode (right)

#### 4.3 Neutron detection test

Following the initial tests to ensure functionality of the GEM detector, the normal cathode was replaced by a 1- $\mu$ m 10B-coated cathode. The detector was then moved to a test station. The layout of the test station is shown in Fig. 9.

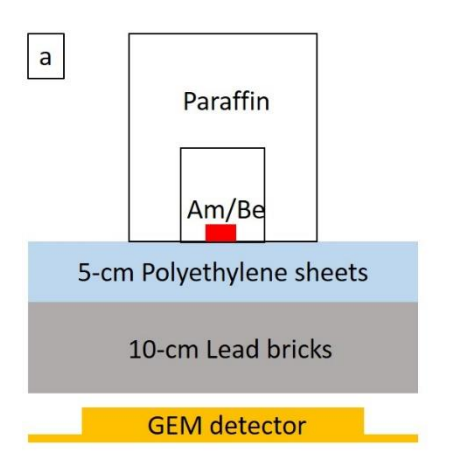




Fig. 9: Neutron test setup

The 5-cm Polyethylene (PE) sheets were used to thermalize fast neutrons from <sup>241</sup>Am/Be, while 10-cm lead bricks were used to shield gamma. The thickness of PE sheets was optimized at 5 cm for the highest yield of thermal neutrons measured using <sup>3</sup>He neutron detector. Also, to ensure the least counts of gamma contributed to neutron counts, a gamma-sensitive Geiger counter was used to measure backgrounds in two cases: with and without <sup>241</sup>Am/Be above the detector. Results showed that no significant differences between two cases were observed, thus 10-cm lead bricks were sufficient for gamma shielding. A gas mixture of Ar/CO<sub>2</sub> (70:30) was flowed through the GEM detector to measure count rates (efficiencies) and signal amplitudes (gains), while varying voltages from -3,900 up to -4,400 V in 50-V increments. To determine the average thermal neutron count rate and signal amplitude for each voltage, 10 sets of 5 minutes long measurement were performed. Counts and amplitudes of signals larger than threshold level (35 A.U.) were used to find average values. After completing all required measurement for a 1-μm <sup>10</sup>B-coated cathode, the cathode was replaced by a 2.5, 3.5, and 4.5-μm <sup>nat</sup>B coated cathodes respectively and all above procedures were repeated.

## 5. Result

## 5.1 Initial functionality test

In order to understand how fast the GEM detector can fully operate after flowing the gas, a test had been done by measuring counts of detection as a function of times. The result is shown in Fig. 10.

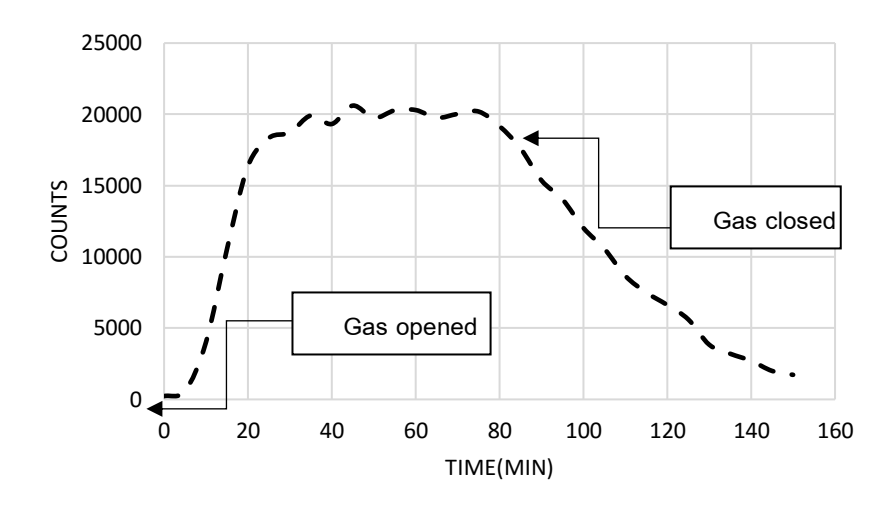


Fig. 10: A plot showing counts of detection as a function of time.

The result had shown that the time required for the detector to fully operate was around 30 minutes while the detector took about 30-40 minutes after closing the gas to reduce its performance by half and took about 70 minutes to completely stop the functionality of the detector.

Since the GEM detector requires gas to continuously flow through the chamber, gas properties could play a major role in defining the detector properties. One property of the gas that is considered vital to radiation detection is its flow rates. In normal operation, the appropriate flow rates, which enable new gas molecules to sufficiently replace depleted gas molecules, should be in the region of 10 times the volume of the chamber per one hour. Since the GEM prototype has approximately 0.3-L chamber, the appropriate flow rate would be 3L/hr. We would like to investigate whether faster flow rates would have effects on the detector with the standard prototyped design shown in Fig. 11 and Fig. 12.

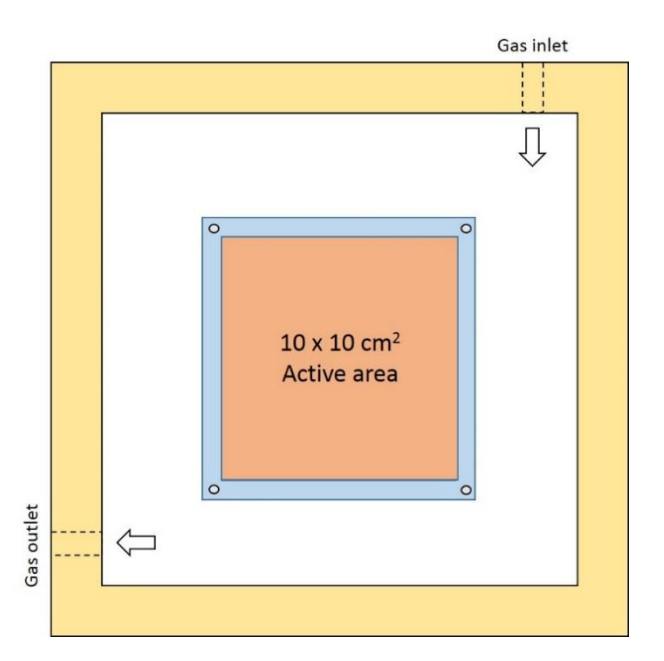


Fig. 11: Top view of the GEM prototype.

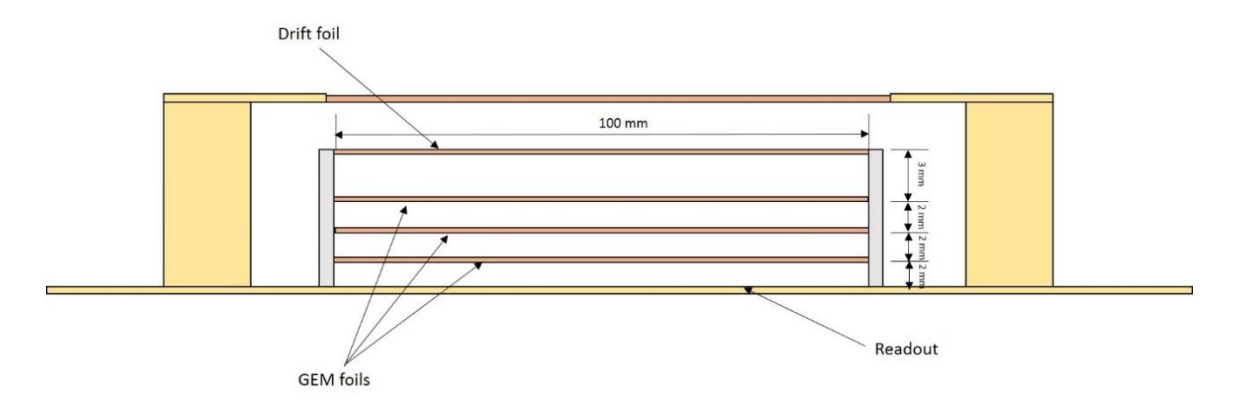


Fig. 12: Side view of the GEM prototype.

In order to investigate the effects of the gas flow rates, active area of the detector was divided into 36 positions. Am-241, which emits 59-keV gamma, was placed on each position for different flow rates (3.0, 4.5, 7.5, and 10.5 L/hr) measured using a direct-read flowmeter and a fixed voltage supply at -4050 V. The number of counts was then used to plot a 3-D contour using OriginPro for uniformity investigation. Results are shown in Fig. 13.

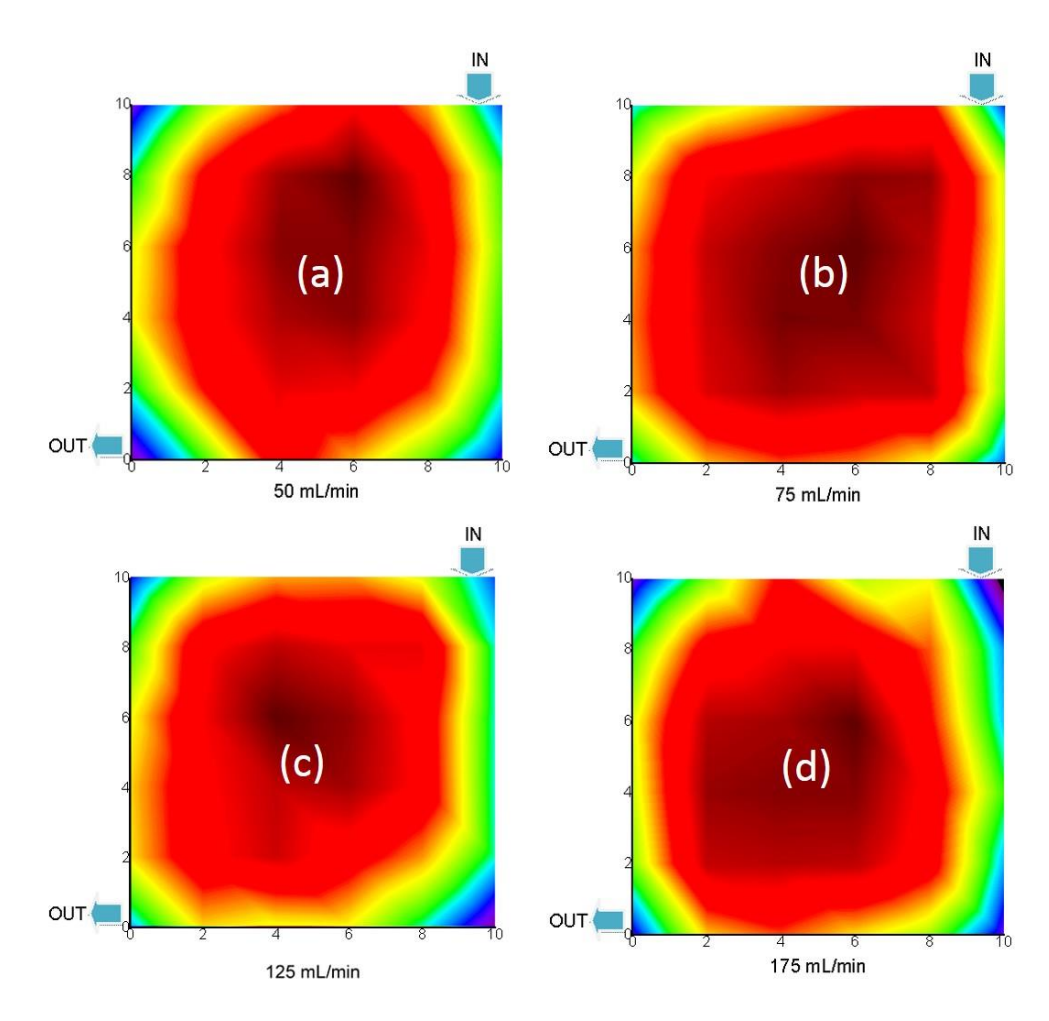


Fig. 13: Results of uniformity test for flow rates: (a) 3 L/hr (b) 4.5 L/hr (c) 7.5 L/hr and (d) 10.5 L/hr

Fig. 13 shows that, even higher flow rates, no significant difference in uniformity was found for a 10 cm x 10 cm GEM prototype. The relative gains and counts at the center of the active area for different gas flow rates (3.0, 4.5, 7.5, and 10.5 L/hr) and different voltage supplied (-3900 V to -4400 V in 50-V increment) were also tested by placing Am-241 at the center of the detector and measuring its counts detected and the average amplitudes of the signals. Results are shown in Fig. 14 and Fig. 15.

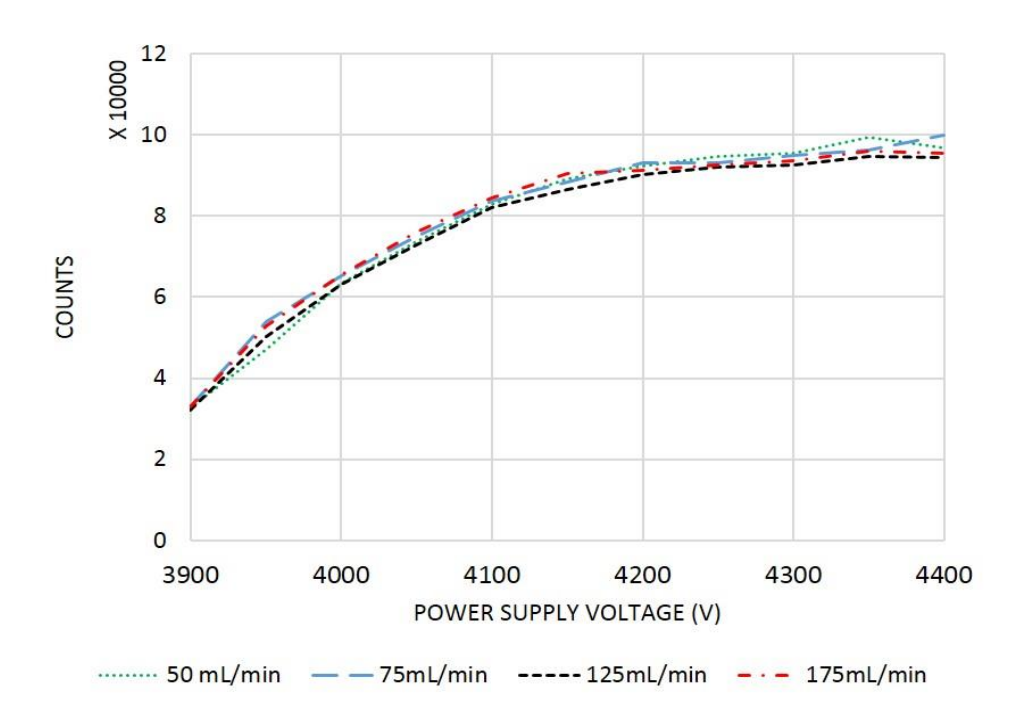


Fig. 14: Results of counts as a function of voltages supplied for different gas flow rates.

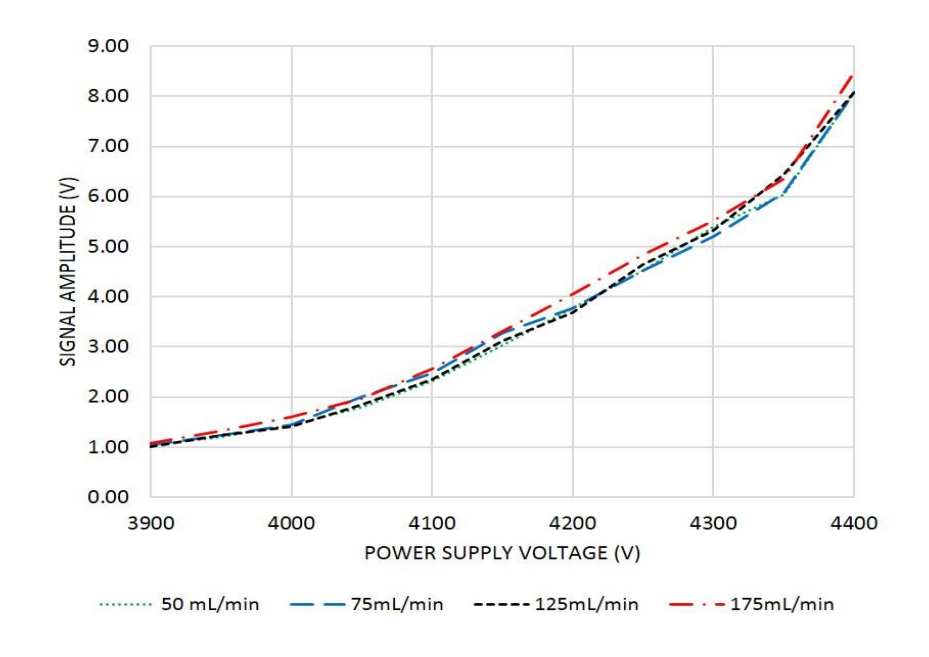


Fig. 15: Results of average amplitude of signals as a function of voltages supplied for different gas flow rates.

Fig. 13-15 show very surprising results as ones might expect changes or non-uniformity in the GEM detector as faster flow rates may create turbulence inside the chamber. However, from a gas flow simulation using COMSOL, it has been shown that the gas flowed above the GEM foils (above active area) is relatively uniform, regardless of flow rates. Results from simulation are shown in Fig. 16.

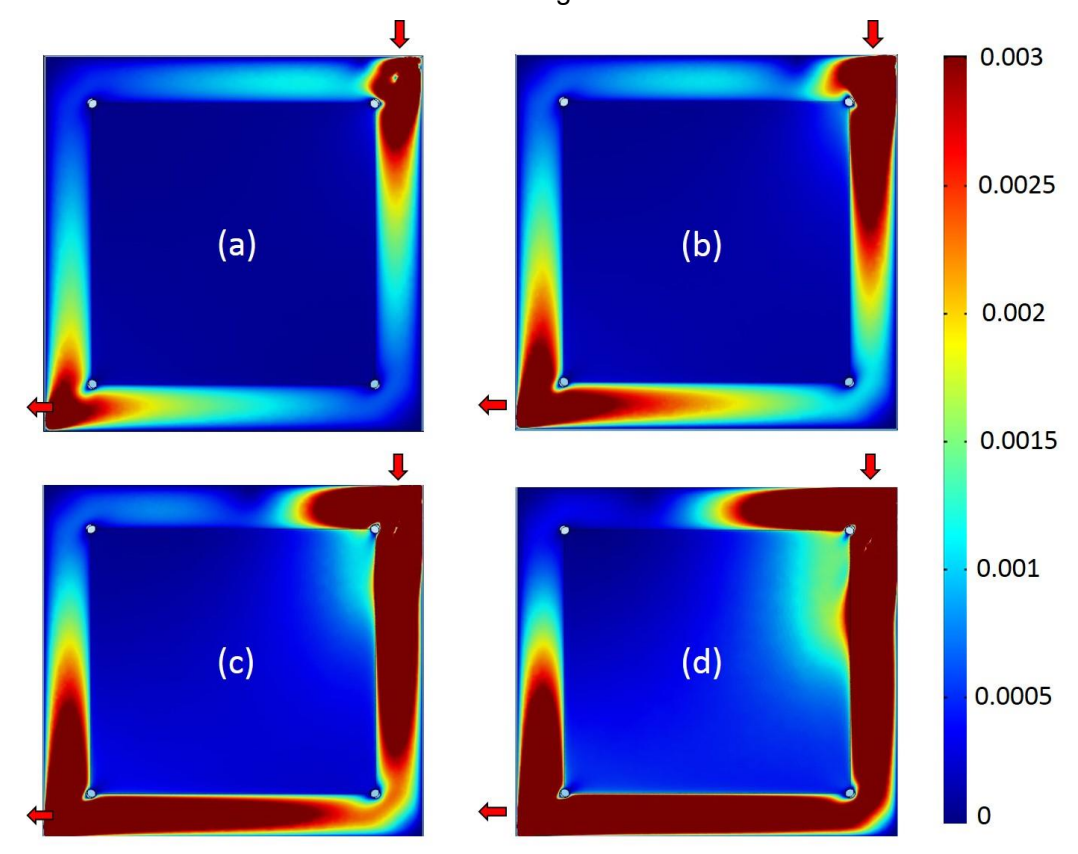


Fig. 16: Results of gas flow simulation inside the GEM detector using COMSOL for flow rates (a) 3 L/h (b) 4.5 L/hr (c) 7.5 L/hr and (d) 10.5 L/hr.

As shown in Fig. 16, the gas distribution at the center of the drift cathode and the topmost GEM foil is relatively uniform and constant for all flow rates simulated. Most of faster gases pass around the active area and possibly create turbulence outside the active area. Hence, once we tested on the uniformity and gains of the detector, they were all relatively the same.

## 5.2 Neutron detection test

For thermal neutron tests,  $1-\mu m^{-10}B$  and 2.5, 3.5,  $4.5-\mu m^{-nat}B$ -coated cathodes were used as neutron converters with Ar/CO<sub>2</sub> (70:30) flowing through the detector. Results of count rates (counts/minute), which represent relative efficiencies, and signal amplitudes, which represent gains of the detector, for each combination are shown in Fig. 17 and Fig. 18.

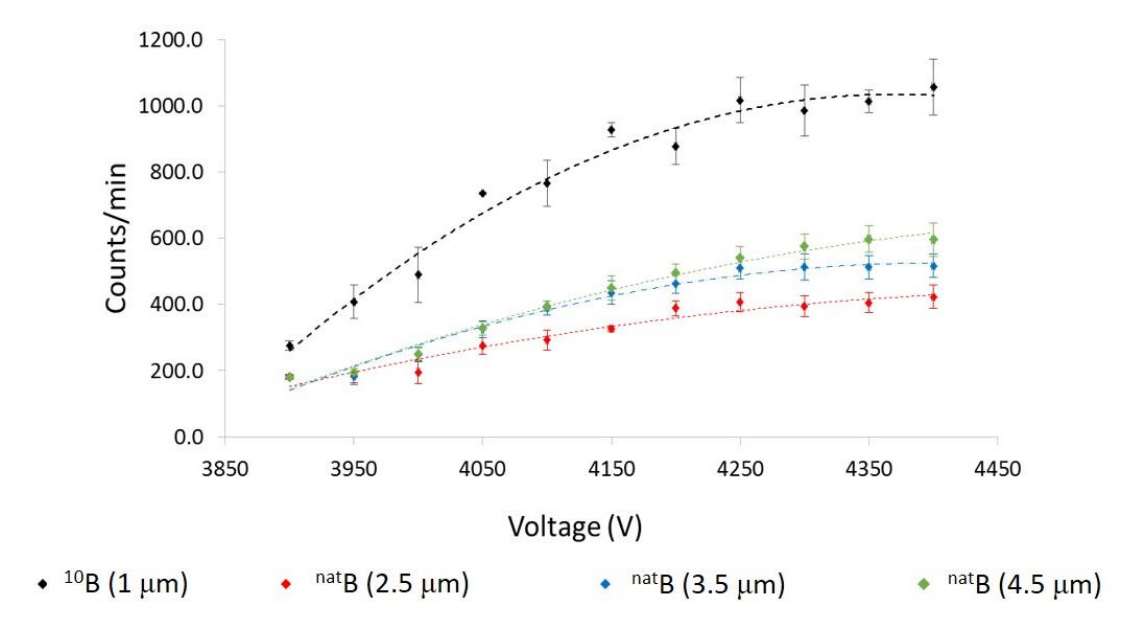


Fig. 17: Count rates of the GEM-based neutron detector

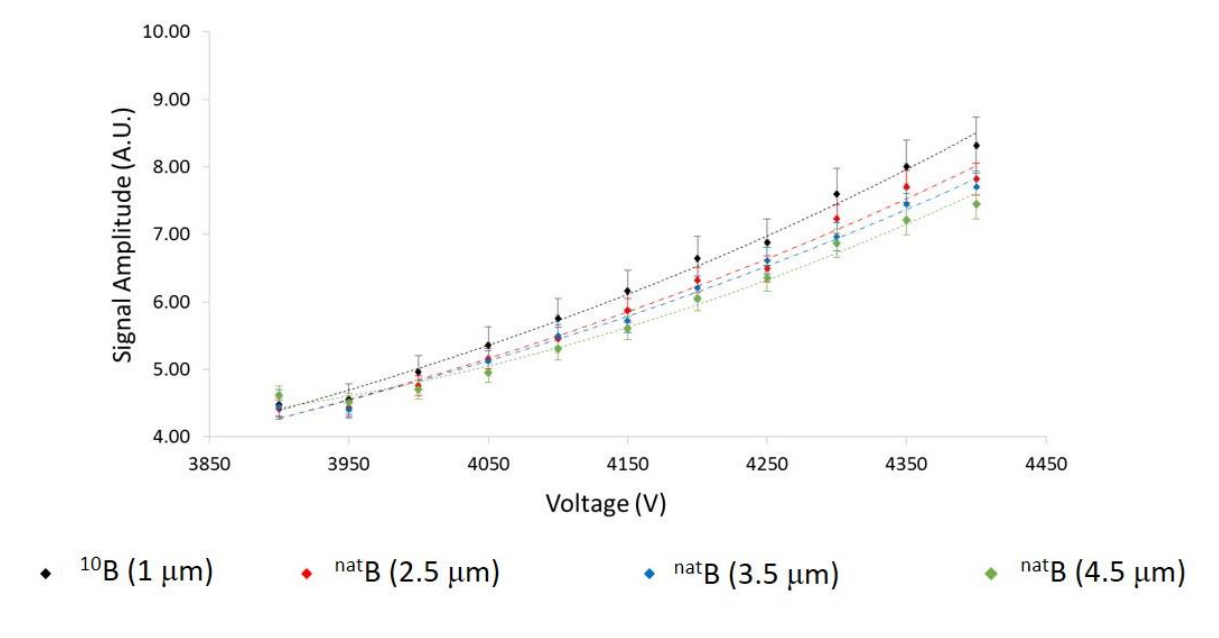


Fig. 18: Signal amplitudes of the GEM-based neutron detector

Fig. 17 shows that thermal neutron count rates increased as voltage supplied increased and reached plateau when the voltage was approximately 4,200 V. Also, the setup, which the cathode was coated by 1-μm <sup>10</sup>B, had the highest count rates compared to any other thickness of <sup>nat</sup>B. This is because <sup>10</sup>B has higher neutron absorption cross section than <sup>nat</sup>B, leading to more interactions between thermal neutrons and boron nuclei. However, as thicknesses of natB increased, the count rates of detection also increased as more <sup>nat</sup>B nuclei were available for interactions. Fig. 18 shows that signal amplitudes increased as voltage supplied increased. The increase in the amplitudes was caused by stronger electric fields inside GEM holes, hence, resulted in more ability to amplify electrons.

#### 6. Conclusion and Discussion

In addition to the ability to detect ionizing particles, the Gas Electron Multiplier (GEM) detector could also be used as thermal neutron detectors. The performance in the detection depends on types of neutron converters applied to the detector, leading to different detection mechanisms. Detection of thermal neutrons relies on nuclear interactions between thermal neutrons and nuclei of neutron converters, which in this research, are either <sup>10</sup>B or <sup>nat</sup>B. The GEM with its cathode coated by 1-µm <sup>10</sup>B had the highest detection count rates, despite its thinnest coating compared to <sup>nat</sup>B. However, as thickness of <sup>nat</sup>B coating increased, the GEM could detect thermal neutrons with higher efficiencies. For gains of the detector, signal amplitudes increased as the supplied voltages increased for all types/thicknesses of boron. These results does not only show capabilities of the GEM detector to detect neutrons but also present ideas and references for researchers to select suitable neutron converters for different applications.

# 7. Appendix

7.1 Manuscript entitled "Recent developments in GEM-based neutron detectors" published on Journal of Physics: Conference series



Recent developments	s in GEM-	based neutre	on detectors
---------------------	-----------	--------------	--------------

This content has been downloaded from IOPscience. Please scroll down to see the full text.

View the table of contents for this issue, or go to the journal homepage for more

Download details:

IP Address: 158.108.27.75

This content was downloaded on 20/05/2015 at 02:28

Please note that terms and conditions apply.

doi:10.1088/1742-6596/611/1/012016

## Recent developments in GEM-based neutron detectors

#### K Saenboonruang1

Kasetsart University, Chatuchak, Bangkok, 10900, Thailand

E-mail: fscikssa@ku.ac.th

Abstract. The gas electron multiplier (GEM) detector is a relatively new gaseous detector that has been utilized for less than 20 years. Since the discovery in 1997 by F. Sauli, the GEM detector has shown excellent properties including high rate capability, excellent resolution, low discharge probability, and excellent radiation hardness. These promising properties have led the GEM detector to gain popularity and attention amongst physicists and researchers. In particular, the GEM detector can also be modified to be used as a neutron detector by adding appropriate neutron converters. With properties stated above and the need to replace the previous expensive <sup>3</sup>He-based neutron detectors, the GEM-based neutron detector could be one of the most powerful and affordable neutron detectors. Applications of the GEM-based neutron detectors vary from researches in nuclear and particle physics, neutron imaging, and national security. Although several promising progresses and results have been shown and published in the past few years, further improvement is still needed in order to improve the low neutron detection efficiency (only a few percent) and to widen the possibilities for other uses.

#### 1. Introduction

On the evening of 8 November 1985, Röntgen noticed that a piece of a cardboard coated with barium platinocyanide showed a faint, flickering, greenish light when electrical discharge took place in a Hittorf-Crookes tube near the cardboard. This observation, which was actually the X-ray detection, led to many inventions and developments of nowadays radiation detectors. The detection capabilities have widened to effectively detect charged particles such as betas, protons and alphas, or even neutral particles such as neutrons which are relatively harder to detect. In particular, the neutron detection has increased its importance in many aspects. One important example is the application of neutron detection in national security. Since plutonium (Pu) and uranium (U) are main ingredients for nuclear weapon enrichment, it becomes international threats if the materials are in terrorist possessions. Since these two elements are amongst other heavy elements that often undergo nuclear fission processes and emit neutrons, one possible and effective way to detect these heavy elements is to have a detector capable of detecting neutrons with high neutron detection efficiency while limiting false alarms from gamma detection. In the past, a helium-3 (3He)-based detector was commonly used due to its high neutron absorption cross section, which leads to high neutron detection efficiency. <sup>3</sup>He is a byproduct from the beta decay of tritium (3H) and is separated from 3H as part of the tritium purification process for refurbishment and dismantlement of the nuclear stockpile. Lately, due to international agreement to reduce numbers of existing nuclear weapons and nuclear stockpiles, the production of 3He from 3H decay has significantly declined and could harm the supply of <sup>3</sup>He for <sup>3</sup>He-based neutron detector. On the other hand, after the terrorist attack on September 11, 2001 in USA, the demand for <sup>3</sup>He has increased

Content from this work may be used under the terms of the Creative Commons Attribution 3.0 licence. Any further distribution of this work must maintain attribution to the author(s) and the title of the work, journal citation and DOI.

Published under licence by IOP Publishing Ltd

<sup>&</sup>lt;sup>1</sup> To whom any correspondence should be addressed.

doi:10.1088/1742-6596/611/1/012016

significantly as <sup>3</sup>He-based neutron detectors were rapidly deployed around the world to detect illegal nuclear materials. These two phenomena lead to the reduction in production and the increase in demand of <sup>3</sup>He. It is estimated that the total <sup>3</sup>He demand is approximately 65,000 liters/year, while the total supply is approximately 15,000 liters/year. These numbers show the disparity between supply and demand of <sup>3</sup>He and a prediction of a more severe shortage of <sup>3</sup>He. In order to maintain national security at the highest level, <sup>3</sup>He-free neutron detectors must be invented to replace the <sup>3</sup>He-based neutron detectors.

In addition to the need of neutron detectors for national security purposes, many scientific and industrial researches also require high-performance neutron detectors. Some examples of research areas that require the uses of neutron detectors include

- Material sciences: The neutron detectors can be used to study and measure the substructures of
  materials and biological organs in the angstrom level by measuring elastic and inelastic
  scattering of neutrons off interested materials.
- Reactor instrumentation: The neutron detectors are used in monitoring power of nuclear power reactor and research reactor since the reactor power is linearly proportional to neutron flux.
- Astrophysics: The neutron detectors can be used to detect secondary neutrons, which are parts
  of the particle showers produced in Earth's atmosphere by cosmic rays.
- Medical imaging: Detection of neutron radiation can be used for medical imaging of patients' organs and tissues.

#### 2. The Gas Electron Multiplier (GEM) detector

The Gas Electron Multiplier (GEM) detector is a gaseous charge amplification structure, invented by F. Sauli and his research group at CERN, Switzerland, in 1997 [1]. The main component of the GEM detector is a thin multilayer foil with many high precision holes, which is known as a GEM foil. The GEM foil consists of a thin insulating foil (polyimide). Polyimide foil has an excellent dielectric strength of 150-300 kV/mm for a thickness of 25-125  $\mu$ m. The usual thickness for polyimide used in GEM foils is 50  $\mu$ m and has metal clads (usually copper) on both sides and perforated with a regular matrix of holes. The holes are very closely spaced and have a diameter ~70  $\mu$ m, and a pitch or a distance from one center of the hole to the center of the closest neighboring holes of ~140  $\mu$ m.



**Figure 1.** A magnified image of a GEM foil shows a regular matrix of holes. Holes have  $\sim$ 70  $\mu m$  in diameter and a pitch of  $\sim$ 140  $\mu m$  [2].

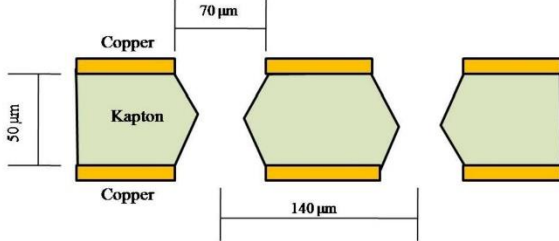


Figure 2. A figure shows a cross sectional view of GEM holes

doi:10.1088/1742-6596/611/1/012016

Another important component of the GEM detector is the gas flushing through the detector. In principle, the GEM detector can be operated in a pure noble gas such as argon (Ar). However, in order to increase the detector stability and to reduce discharge probability, a mixture of gasses is used. The standard gas mixture used in most applications is a mixture of Ar/CO<sub>2</sub> in a ratio of 70/30, where Ar acts as the main ionizing gas and CO<sub>2</sub> acts as a quencher.

The main operating principles of the GEM detector are as the following steps.

- By applying a potential difference about 300-400 V between the top and the bottom metal clads, strong electric fields develops inside the holes.
- A particle passes through the drift region of the detector and ionizes gas molecules inside the
  detector. These ionized electrons will then travel through the strong electric fields inside the
  GEM holes, gain more energy, and ionize other gas molecules creating electron avalanches.
- In the last amplification stage, the amplified electron avalanches will be captured by readout
  pads or readout strips depending on the applications. The moving of electron avalanches
  between the last GEM foil and the readout electrode will create detectable signals, which will
  be processed through an appropriate data acquisition (DAQ) system.

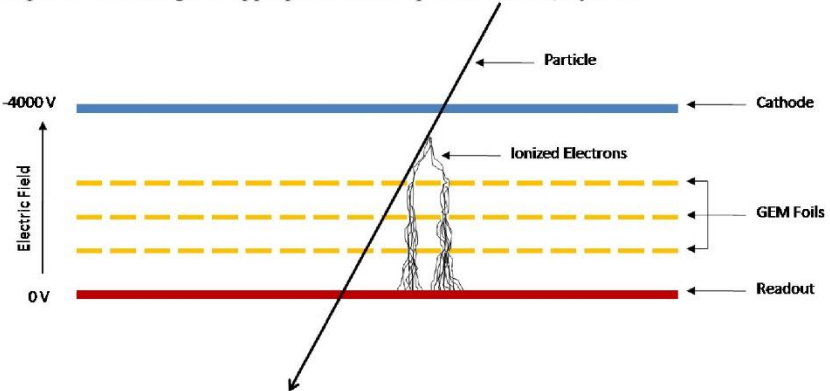


**Figure 3.** The picture shows the three amplification stages inside the GEM detector. The last electron avalanches will be captured by the readout pads or the readout strips. The moving of electron avalanches between the last GEM foil and the readout electrode will create detectable signals and will be processed through DAQ system.

## 3. GEM detector as a neutron detector

Although the GEM-based detector is mostly used to detect charged particles and low-energy photons, the detector can be modified by adding appropriate neutron converters to the detector such that it is now able to detect neutrons. The ability to detect neutrons relies on a conversion mechanism that yields charges in the drift volume of the detector. In the case of thermal neutrons, conversion takes place via a nuclear reaction with an appropriate isotope, while higher energy neutrons may cause nuclear recoils. To increase the probability of the conversion, an appropriate neutron converter is added to the detector. Examples of commonly used neutron converters include Helium-3 ( $^3$ He ), boron-10 ( $^{10}$ B), lithium-6 ( $^6$ Li) or hydrogen-rich materials such as polyethylene (( $(C_2H_4)_nH_2)$ ) and polypropylene (( $(C_3H_6)_n$ ). The nuclear reaction products are an alpha ( $\alpha$ ) particle of  $\sim$ 2 MeV and either a triton (for  $^6$ Li) or lithium ion (for  $^{10}$ B), isotropically emitted in opposite directions. Example of the nuclear reaction with  $^{10}$ B can be shown as the following:

$$^{10}$$
B + n  $^{-10}$ B + n  $^{-10}$ B + n  $^{-10}$ B + n  $^{-10}$ B +  $^{-10}$ B

doi:10.1088/1742-6596/611/1/012016

where <sup>7</sup>Li\* is an excited particle. The <sup>7</sup>Li\* spontaneously emits a 0.48 MeV gamma ray and returns to the ground state. These emitted alpha particles will ionize gas molecules inside the GEM detector, which will later be amplified in the amplification stages and get captured by readout pads. The efficiency of neutron detection depends on the neutron reaction rate which also depends on various factors. The neutron reaction rate is shown in (3.1).

$$R = \int \phi(E) N \sigma(E) dE \tag{3.1}$$

where  $\emptyset = \int \emptyset(E) dE$  is the neutron flux, N is the number of  $^{10}$ B atoms in the neutron converter, and  $\sigma(E)$  is the neutron cross section. The value of neutron cross section is the most important quantity that defines the efficiency of the detector and is shown in figure 4.

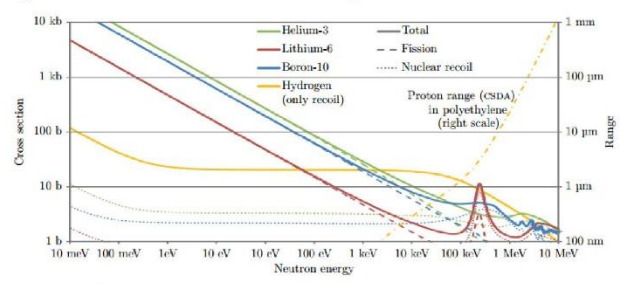


**Figure 4.** Cross sections of selected elements used as neutron converters. Dashed and dotted curves decompose the total interaction cross section from nuclear reaction and nuclear recoil reactions [3].

As shown in figure 4, <sup>3</sup>He has the highest cross section and has been used widely for neutron detectors in the past. Due to a crisis in the shortage of <sup>3</sup>He and the sharp increase in the price of <sup>3</sup>He, alternatives to <sup>3</sup>He-based neutron detectors are urgently needed to maintain the highest level of national security and researches. These include the uses of thin film coated with <sup>10</sup>B or <sup>6</sup>Li, or filling the detector with hydrogen-rich gas.

#### 4. Recent development and result

Since the invention of the GEM detector, the growing interests in its capabilities have motivated scientists and researchers to develop and improve the detector for various applications. GEM-based neutron detector is one of applications that have been vastly developed in recent days. Some of the notable developments and results will be discussed in this section.

## 4.1 Manufacturing of boron-coated GEM foil

Since the performances of the GEM-based neutron detector especially the efficiency of the detection depend heavily on the neutron converting process occurred at the converters, the development of methods to apply converters (<sup>10</sup>B) to drift cathode and GEM foils is very important. As shown by Se-Hwan Park *et al.* [4,5], <sup>10</sup>B was coated on the aluminized Mylar, which was used as a drift cathode, using electron-beam evaporator. The coated boron became stable with time. However, <sup>10</sup>B did not adhere to the GEM foil very well and could be peeled off as well as cracked easily from the GEM foil. The picture of borated GEM foil that peeled off is shown in figure 5.

doi:10.1088/1742-6596/611/1/012016

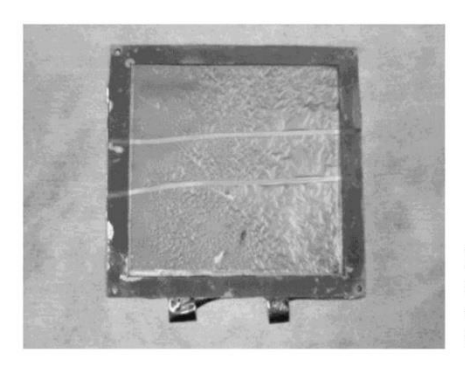


**Figure 5.** Boron coated on the GEM foil using electron-beam evaporator done by Se-Hwan Park *et al.* could be easily peeled off after the process. Image was taken from [5].

Se-Hwan Park *et al.* had solved the problem by, instead of coating one full piece of  $^{10}$ B film on the GEM foil, the  $^{10}$ B film was segmented into small squares. To achieve that, the main additional procedure included the introduction of a stainless mesh placed in front of the substrate so that the  $^{10}$ B films were divided into  $\sim 1.5 \text{ x } 1.5 \text{ cm}^2$  squares and had the gap between the adjacent squares of 0.3 mm. Pictures of drift cathode and GEM foil that were coated with the new procedure are shown in figure 6.

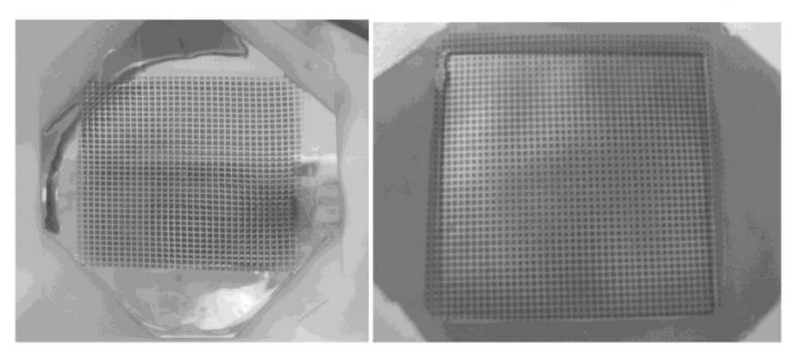


**Figure 6.** Pictures of <sup>10</sup>B-coated drift cathode (GEM foil) is shown on the left (right). Images were taken from Se-Hwan Park *et al.* [4,5].

The idea of segmenting <sup>10</sup>B film into small squares reduced the stress on the film surface significantly and even if the crack occurred, the crack remained in the broken square and did not spread to other parts. The technology has improved the manufacturing of the <sup>10</sup>B-coated GEM foil and significantly improved qualities of GEM-based neutron detector. Furthermore, the technique has increased the working duration of the foil and the detector.

#### 4.2 Improvement on the configuration and layout of the converter

Since the ability to detect neutrons depends on the ability to convert neutrons to charged particles such as alphas or protons, the way the converter is introduced to the detector is highly important to the performances of the detector. In a traditional configuration, the converters such as <sup>10</sup>B and polyethylene are coated directly onto the drift cathode and the GEM foils. However, this method of applying converters limits the conversion process to only at the surface of the detector. Furthermore, even if the thickness of the converter increases which would increase the conversion probability, charged particles produced cannot penetrate the thick converter. Hence, the thickness of the converter is limited to only

doi:10.1088/1742-6596/611/1/012016

 $2-3 \mu m$  in the case of  $^{10}B$ . A. Pietropaolo *et al.* [6] has designed a new GEM-based neutron detector to remove these constraints by introducing layers of borated glass sheets as converters that are perpendicular to the drift cathode as shown in figure 7.

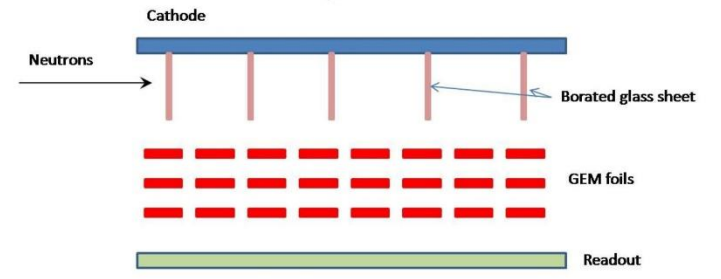


**Figure 7.** Schematic of GEM-based neutron detector designed by A. Peitropaolo *et al.*: The borated glass sheets were applied perpendicular to the drift cathode [6].

The main purpose of having layers of borated glass sheet aligned as in figure 7 is to loosen up the requirement that neutrons must be converted to charged particles at the very first µm-thick surface of the detector. The improvement consequently increases the probability of the conversion and, hence, the efficiency of the detector. The efficiency measured by A. Pietropaolo *et al.* showed that the efficiency of the neutron detection came out to be 4.8(5) % which was much better than previously reports of traditional configurations, which had the efficiency of less than 1%. A similar design was also used in the research conducted by M. Cortesi *et al.* [7] for fast neutron detection, which used polyethylene (HPDE) layers as converters. The reports showed that the estimated efficiency that could be achieved by this configuration was in the range of 5-8 % for 2.5 MeV neutrons.

## 5. Possible improvement and application

Although growing number of tests and researches have been conducted on the GEM-based neutron detector, there are still rooms for further improvement such as:

- Conducting extensive researches on various neutron converters including gaseous converters such as He-4 and other solid converters (<sup>6</sup>Li), or a mix of both solid and gaseous converters used in the detector.
- Designing new layouts of converters such that there are more possibility of conversion. This
  might include adding more layers of borated glass sheets to the detector.

Since many reports have shown the excellences of the GEM-based neutron detector, more researches should be aimed to adapt the detector for applications. One example of applications was done by S. Uno *et al.* The GEM-based neutron detector was used to perform a 2-dimensional imaging of metal content, which could clearly show content of gold in a Japanese oval gold coin from Edo period. Furthermore, the detector could also be used to perform a 2-dimensional imaging of crystallite size of iron bars after bending [8][9]. These examples clearly show the wide areas of applications of the GEM-based neutron detectors and there are still plenty of rooms to explore.

#### 6. Conclusion

The GEM detector has been development significantly since the invention in 1997. From the ability to detect charged particles and photons, the GEM detector has been adapted to be used in various applications. Neutron detector based on the GEM detector is one of the detection technologies that greatly benefit educational, industrial, medical, and national security sectors. Many research projects have been conducted to improve the performances of the detector. These include the attempts to improve the method to apply converters to the drift cathode and the GEM foils such that the converters could adhere to the surface better and increase the lifetime of the detector. Also, researchers have designed

doi:10.1088/1742-6596/611/1/012016

new arrangements of the converters to improve the chances of the conversion by adding layers of borated glass sheets or HDPE perpendicular to the drift cathode. This design has increased efficiency of the detector to be in the range of 5%, which improves from previously reports of ~1%. Furthermore, attempts to adapt the GEM-based neutron detector to be used in various applications such as in material analysis, medical imaging, and national security should be emphasized and invested.

#### Acknowledgments

This work was supported by the Thailand Research Fund (TRG5780292) and Kasetsart University Research and Development Institute. Additional support was provided by Faculty of Science, Kasetsart University. I also would like to express my appreciation to Dr. Nilanga K. Liyanage (University of Virginia) and Dr. Thiraphat Vilaithong (Thailand Center of Excellence in Physics) for their useful advices.

#### References

- [1] Sauli F 1996 A new concept for electron amplification in gas detectors *Nucl. Instr. and Meth. A.* 386 531–34
- [2] Sauli F 2004 Progress with the gas electron multiplier Nucl. Instr. and Meth. A. 522 93-98
- [3] Pinto S D 2013 GEM applications outside high energy physics *Mod. Phys. Lett. A.* **28** 1340025
- [4] Park S H, Kim Y K and Kim J K 2005 Neutron detection with a GEM IEEE Transactions on Nuclear Science. 52(5) 1689–92
- [5] Park S H, Kim H S, Ha J H, Kim Y K and Kim J K 2006 Fabrication of a GEM-based gas detector for thermal neutron measurement J. Korean Phys. Soc. 49(5) 1939–43
- [6] Pieotropaolo A et al2013 A new <sup>3</sup>He-free thermal neutrons detector concept based on the GEM technology Nucl. Instr. and Meth. A. 729 117–26
- [7] Cortesi M, Zboray R, Adams R, Dangendorf V and Prasser H M 2012 Concept of a novel fast neutron imaging detector based on THGEM for fan-beam tomography applications JINST 7 C02056
- [8] Uno S et al 2012 Two-dimensional neutron detector with GEM and its applications Physics Procedia 26 142-52
- [9] Uno S et al 2012 Development of a two-dimensional gaseous detector for energy-selective neutron radiography Physics Procedia 37 600–05

7.2 Manuscript entitled "Investigation on Properties of the 10 cm  $\times$  10 cm GEM Prototype" which is currently under review for publication on Maejo International Journal of Science and Technology.

Full paper

# Investigation on Properties of the $10 \text{ cm} \times 10 \text{ cm}$ GEM Prototype

Kiadtisak Saenboonruang<sup>1,\*</sup>, Piyakul Kumphiranon<sup>1</sup>, Kittipong Kulasri<sup>1</sup> and Anawat Ritthirong<sup>1</sup>

<sup>1</sup>Department of Applied Radiation and Isotopes, Faculty of Science, Kasetsart University, Bangkok, 10900, Thailand

Corresponding author, e-mail: fscikssa@ku.ac.th, k.saenboonruang@gmail.com

Abstract: The Gas Electron Multiplier (GEM) detector is one of promising particle and radiation detectors that has been improved greatly from previous gas detectors. The improvement includes better spatial resolutions, higher detection rate capabilities, and flexibilities in designs. In particular, the 10 cm × 10 cm GEM prototype was utilized in various applications including high resolution tracking devices in nuclear and particle physics. With its simplicity in operations and designs, while still maintaining high qualities, the GEM prototype was suitable for both start-up and advanced researches. This article reports the procedures and results of the investigation on important properties of the 10 cm × 10 cm GEM detector using current measurement and signal counting. Results had shown that gains of the GEM prototype exponentially increased as the voltages supplied to the detector increased, while the detector reached full efficiency (plateau region) when the voltages were greater than -4100 V. In terms of signal sharing between X and Y strips of the readout, X strips, which was on the top layer of the readout, collected larger signal (~57%). For the uniformity test, the GEM prototype had slightly higher efficiencies at the center of the detector. These results could be used for future references and for better understanding in the GEM prototype's characteristics.

**Keywords** GEM, Particle detector, Radiation, Gas Electron Multiplier

1

#### INTRODUCTION

The Gas Electron Multiplier (GEM) detector was invented by F. Sauli in 1997 [1]. Since the invention, the GEM detector has gained attentions amongst international scientists and researchers. Parts of the success are from its improved properties from previous gas detectors. Examples of the improvements are [2]:

- the ability to operate in most gases
- the ability to vary gains of the detector (up to 10<sup>5</sup>)
- excellent spatial resolution (50 μm or better) [3]
- high rates capability (10<sup>5</sup> Hz/mm<sup>2</sup>)
- flexibilities in designs
- · relatively low cost

The GEM detectors are now utilized in various scientific researches including tracking devices in nuclear and particle physics [4], medical imaging [5], astronomy [6], and neutron detection [7].

The 10 cm × 10 cm GEM prototype is designed, developed, and supplied by the Gas Detectors Development Group (GDD) at CERN. The triple GEM prototype consists of three GEM foils, which are 50-µm thin insulating foils made of polyimide (Kapton). Each foil is sandwiched by two thin copper plates. The GEM foil is perforated with arrays of 70-um diameter holes (GEM holes) with 140-µm pitches between two adjacent holes. Voltage difference of 250-400 V is supplied between the two copper plates such that strong electric fields are formed inside the GEM holes. In addition to GEM foils, the drift cathode is usually made of a thin sheet of aluminized Kapton, where the aluminum side is supplied with the most negative voltage. All GEM foils and the drift cathode are enclosed in a gas-tight box with one gas inlet and one gas outlet. Readout of the GEM prototype has the XY configuration where two sets of 512 thin conducting wires running perpendicular to each other in X and Y directions. The schematic drawings of the GEM prototype and the readout strips are shown in Figure 1 and Figure 2. The widths of the X and Y strips are 50 µm and 150 µm respectively. The difference in strip widths is designed to improve signal sharing between X and Y strips. To operate the GEM detector, appropriate gas filling must flow through the detector. In principle, a pure noble gas such as argon (Ar) can be used. However, in order to improve the stability of the detector, a gas mixture is usually used. The standard gas mixture to operate the GEM detector is Ar/CO<sub>2</sub> with the ratio of 70:30. Ionizing particles and radiation passing through the GEM detector will ionize gas molecules inside the detector and create groups of primary electrons. These primary electrons will drift down to GEM foils and gain enough energy from strong electric fields inside GEM holes to further ionize gas molecules. The amplified signal will be detected by XY readout strips and transferred to appropriate Data Acquisition system (DAQ) for data processing [8].

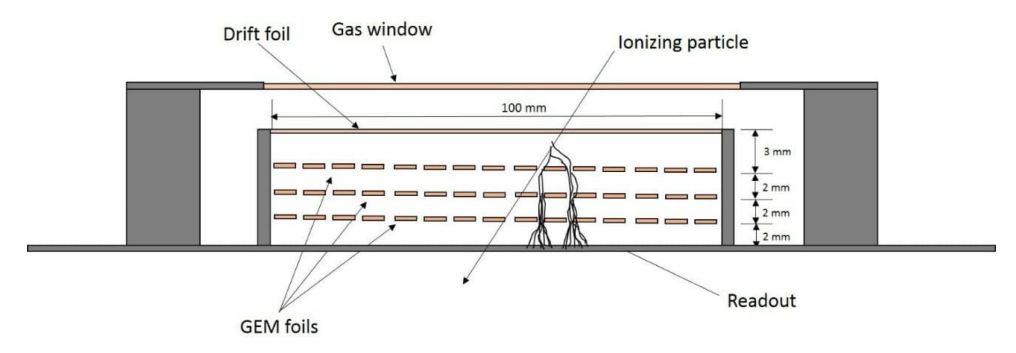


Figure 1. The schematic drawing of the  $10 \text{ cm} \times 10 \text{ cm}$  GEM prototype. GEM foils and drift cathode are stacked at the center of the gas-tight box with the readout serving as the base of the detector

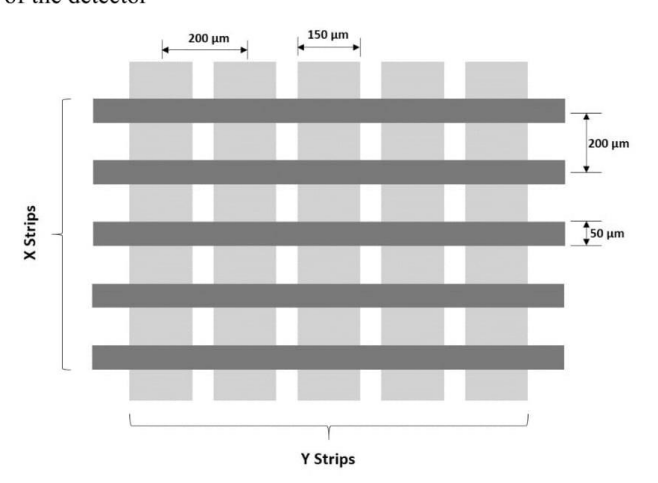


Figure 2. The schematic drawing of the readout of the 10 cm  $\times$  10 cm GEM prototype in XY configuration. The X strips are wires that are on top with the strip width of 50  $\mu$ m and

a distance between strips of 200  $\mu m$ . The Y strips are bottom wires with the strip width of 150  $\mu m$  and a distance between strips of 200  $\mu m$ 

The GEM technology has been developed greatly in recent years. Sophisticated designs and large-sized detectors have been manufactured to be used in many advanced researches. In particular, the 10 cm × 10 cm GEM detector plays important roles in many researches, especially start-up researches and preliminary studies. However, information and simple procedures of the detector's performances are still inadequate. Hence, this article aims to report thorough details of the procedures, calculations, and results of the investigation on important properties of the detector: the plateau behavior of the detector, gains of the detector as a function of the power supply voltages, signal sharing between X and Y strips, and the uniformity of the detector.

#### 2. MATERIALS AND METHODS

#### Plateau investigation

To investigate plateau region of the GEM prototype, 5.9-keV X-ray emitted rate from Fe-55 were measured as voltages of power supply varied from -3900 to -4300 V in 50-V increments. Setup schematic diagram of the rate measurement is shown in Figure 3. The preamplifier used for this purpose was a charge sensitive amplifier (Cremat-110) with ×4 amplification [9]. The threshold at the discriminator was set at 65 mV to eliminate all electronic noises. The power was supplied to the GEM prototype through a voltage divider shown in Figure 4.

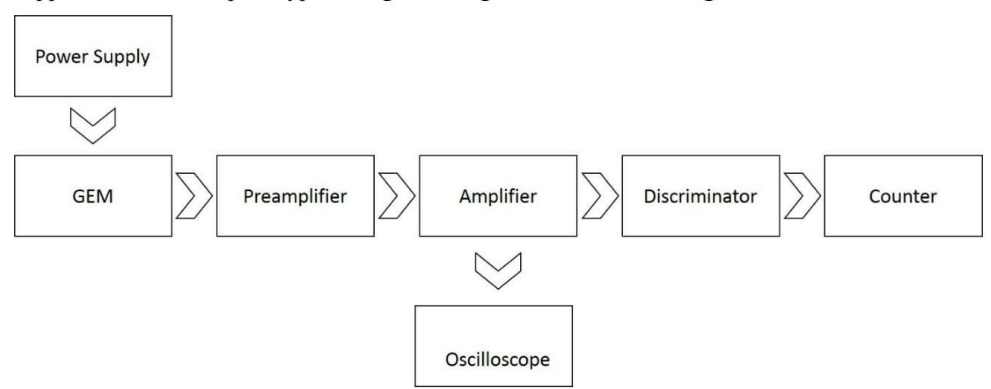


**Figure 3.** The figure shows schematic drawing of the setup for the rate measurement in the plateau investigation

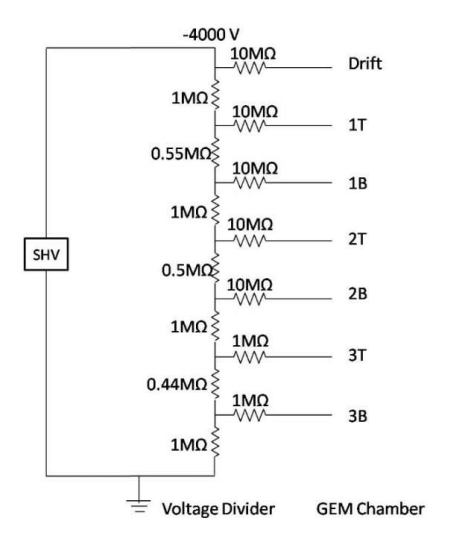


**Figure 4.** The figure shows the schematic drawing of the voltage divider used for supplying voltages to the GEM prototype

#### Gain measurement

To measure gains of the GEM prototype, currents passing through the readout after the amplification from 5.9-keV X-ray emitted from Fe-55 were measured as voltages of power supply varied from -3900 to -4300 V in 50-V increments.

From the equation

$$I = R \times N \times G \times e \tag{1}$$

where I is the current, R is the rate of the 5.9-keV X-ray from Fe-55, N is the number of primary electrons, G is the gain of the detector, and e is the charge of an electron ( $e = 1.6 \times 10^{-19}$  C). In order to obtain G, values of I, R, and N must be carefully measured and evaluated. To measure I, a pico-ammeter which has a 20-fm current resolution was used for the current measurement. The setup for the current measurement is shown in Figure 5. R was the value of the rate of 5.9-keV X-ray emitted from Fe-55 at the plateau region. N could be estimated using the average work function (W) of the gas mixture (Ar/CO<sub>2</sub>) in the ratio of 70:30. The average W was calculated using Eq. 2.

$$\frac{1}{W} = \frac{of\ Ar}{W_{Ar}} + \frac{of\ CO_2}{W_{CO_2}} \tag{2}$$

where  $W_{Ar} = 25$  eV,  $W_{CO2} = 34$  eV, % of Ar = 0.7, and % of  $CO_2 = 0.3$ . Using these values in Eq. 2 gave W = 27.8 eV [10]. Assuming that only photoelectric effect occurs during the interaction between X-ray and gas molecules, the value of N would be approximately 212 electrons.

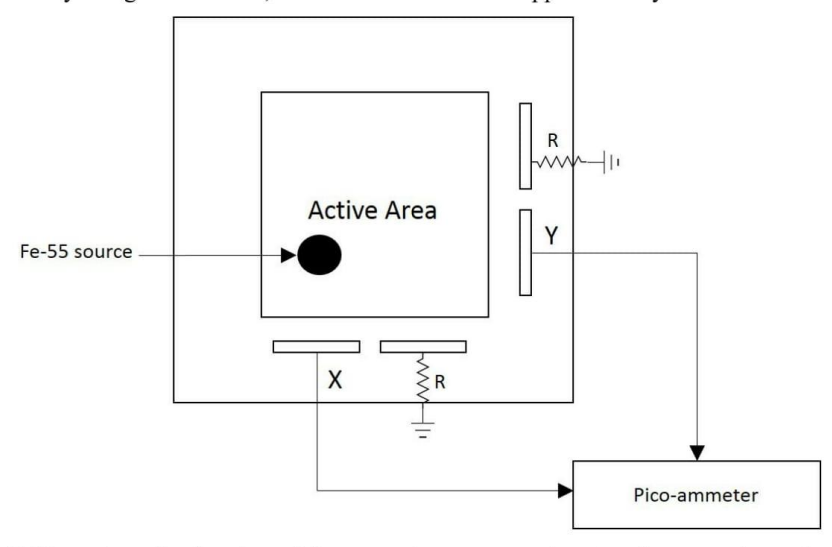


**Figure 5.** The schematic drawing of the current measurement using pico-ammeter and a Fe-55 source. Two scenarios: only X strips and a combination of X and Y strips, were used for current measurement

#### Signal sharing between X and Y strips

Although the purpose of the different widths in the XY readout strips is to improve signal sharing between X and Y such that equal signals are shared between them, inequality in the signal sharing could still occur. To investigate the signal sharing, currents were measured in two scenarios; only X strips ( $I_1$ ) and a combination of X and Y strips ( $I_2$ ). The ratio of  $I_1/I_2$  indicates percentages of the signal collected by X strips.

#### Uniformity test

Since efficiencies of the GEM detector at areas near edges of the active area are expected to be lower than efficiencies at the center of the active area, investigation of the uniformity of the

GEM detector is needed to better understand these differences. To test the uniformity, the 10 cm  $\times$  10 cm active area was divided into 36 positions (6 columns and 6 rows). Am-241, which emits primary alpha particles and 59-keV secondary gamma, was placed on each position. In order to correctly compare efficiencies from different positions, gas flow rate (3.0 L/hr), detection duration (3 minutes), and power supply voltage (-4100 V) were set to be the same throughout the measurement. For each position, numbers of counts detected using the setup in Figure 3 were collected and averaged. After completing all 36 positions, numbers of counts were plotted using the OriginPro software to produce a contour of uniformity.

## RESULTS AND DISCUSSION

### Plateau investigation

Results of count rates as a function of power supply voltages are shown in Table 1 and Figure 6.

Table 1. Count rates of the GEM prototype as the power supply voltages varied

Count Rate (Hz)
270
501
611
647
665
658
665
676
673

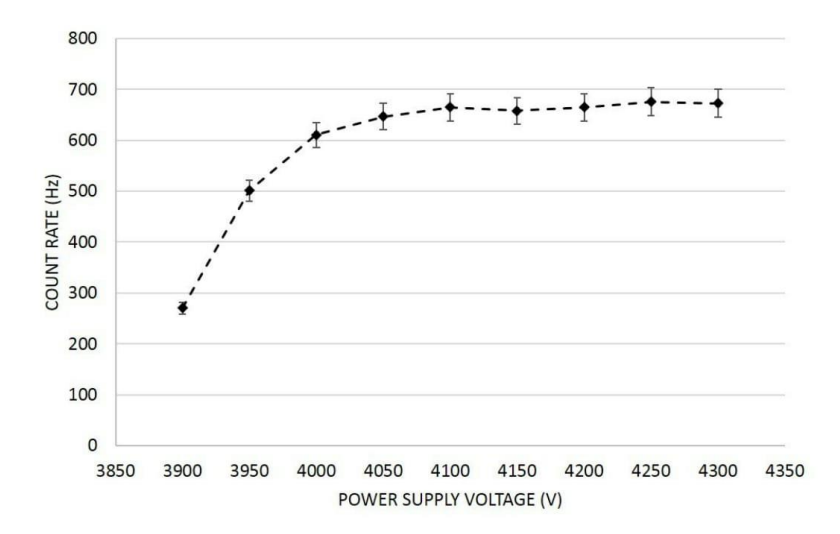


Figure 6. Figure shows count rates of the GEM prototype as a function of power supply voltages. The GEM prototype reached plateau region after  $\sim$ 4100 V.

As shown in Figure 6, the full efficiency (plateau region) of the GEM prototype occurred when the power supply voltages were higher than  $\sim$  -4100 V. This implies that even though amplitudes of signals became larger as the voltages increase, the full efficiency of the GEM prototype was already achieved at V = -4100 V.

#### Gain measurement

From previous calculations and results,  $R \sim 670$  Hz, N = 212 electrons, and  $e = 1.6 \times 10^{-19}$  C. The current values with a combination of X and Y strips as a function of power supply voltages are shown in Table 2.

Table 2. Currents of the GEM prototype as the power supply voltages varied

Current (nA)
0.05
0.07
0.10
0.15
0.20
0.29
0.42
0.60
0.90

With values of I, N, e, and R indicated in previous section, gains for different voltages were calculated and are shown in Table 3 and Figure 7.

Table 3. Gains of the GEM prototype as the power supply voltages varied

Power Supply Voltage (V)	Gain
3900	2200
3950	3080
4000	4400
4050	6600
4100	8800
4150	12760
4200	18480
4250	26401
4300	36901

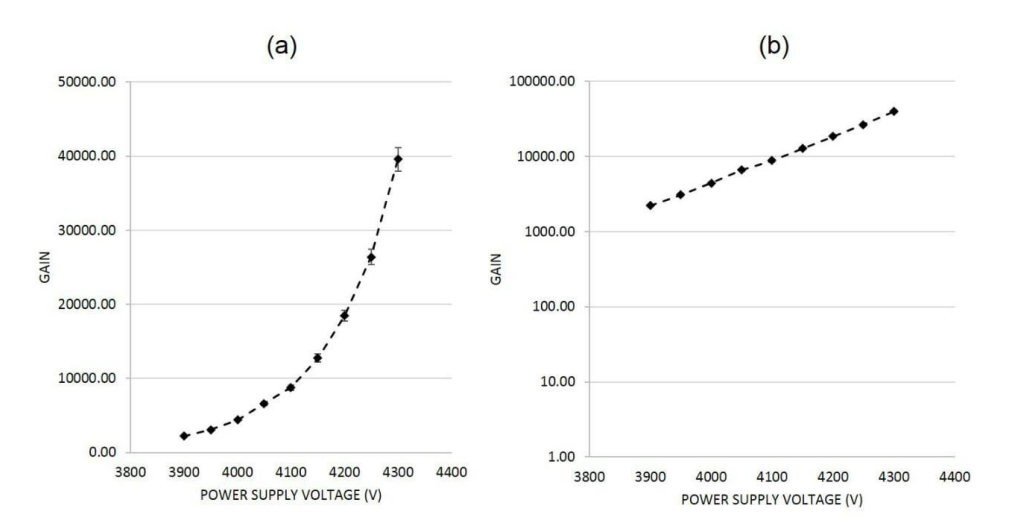


**Figure 7.** Figures (a) and (b) show gains of the GEM prototype as power supply voltages varied. Figure (b) is plotted in logarithm scale.

As shown in Figure 7(a) and Figure 7(b), gains of the GEM prototype exponentially increase as the power supply voltages increase.

## Signal sharing between X and Y strips

To determine ratio of signal sharing between X and Y strips, currents from X strips only  $(I_1)$  were compared with currents from a combination of X and Y strips  $(I_2)$ . Values of currents from both scenarios are shown in Table 4. Values of  $I_1/I_2$  are plotted in Figure 8.

Table 4. Current measurement from X strips only and a combination of X and Y strips

	1 2			
Power Supply	Current from	Current from	$I_1/I_2$	
Voltage (V)	X Strips, $I_{l_i}$ (nA)	A combination of		
		X and Y strips, $I_2$ ,		
		(nA)		
3900	0.03	0.05	0.60	
3950	0.04	0.07	0.57	
4000	0.06	0.10	0.60	
4050	0.08	0.15	0.53	
4100	0.12	0.20	0.60	
4150	0.16	0.29	0.55	
4200	0.25	0.42	0.60	
4250	0.33	0.60	0.55	
4300	0.51	0.90	0.57	

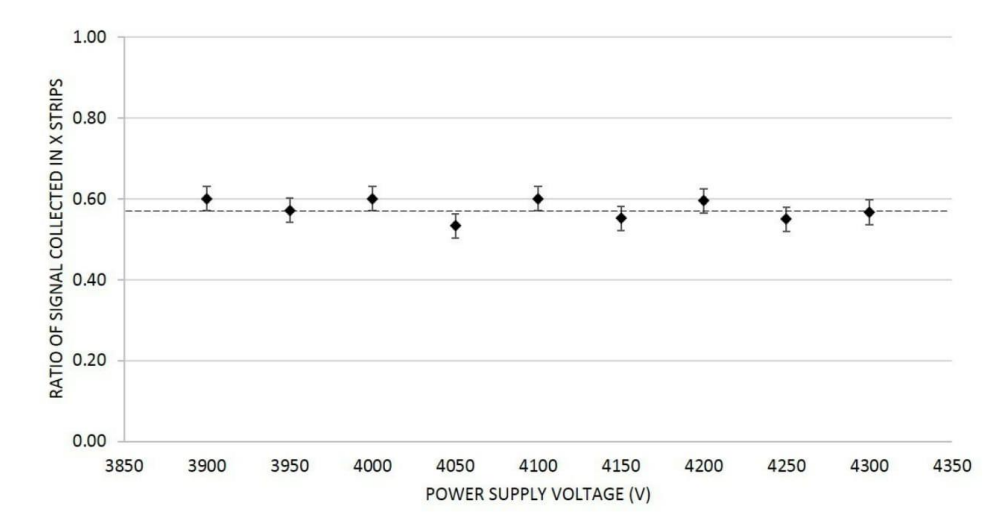


**Figure 8.** The figure shows ratios of  $I_1$  and  $I_2$ . The dotted line is the average of all ratios, which is  $0.57\pm0.03$ .

Figure 8 shows that the average  $I_1/I_2 = 0.57\pm0.03$ . Hence, the X trips, which were narrower and located on the top layer of the readout, collected larger signals compared to Y strips. To improve better signal sharing, a new design and better manufacture of the readout are required [4].

## Uniformity test

Figure 9 shows the uniformity of the GEM prototype using Am-241 as a gamma emitter. Areas near the center of the active area had higher efficiencies compared to areas near edges. This behavior was expected since ionizing particles or ionized electrons occurred near edges had possibilities to travel or drift out of the active area, and thus, lower its overall efficiencies and signal amplitudes. However, if considering areas with at least 1 cm away from edges, the efficiencies were well within 20% from each position.

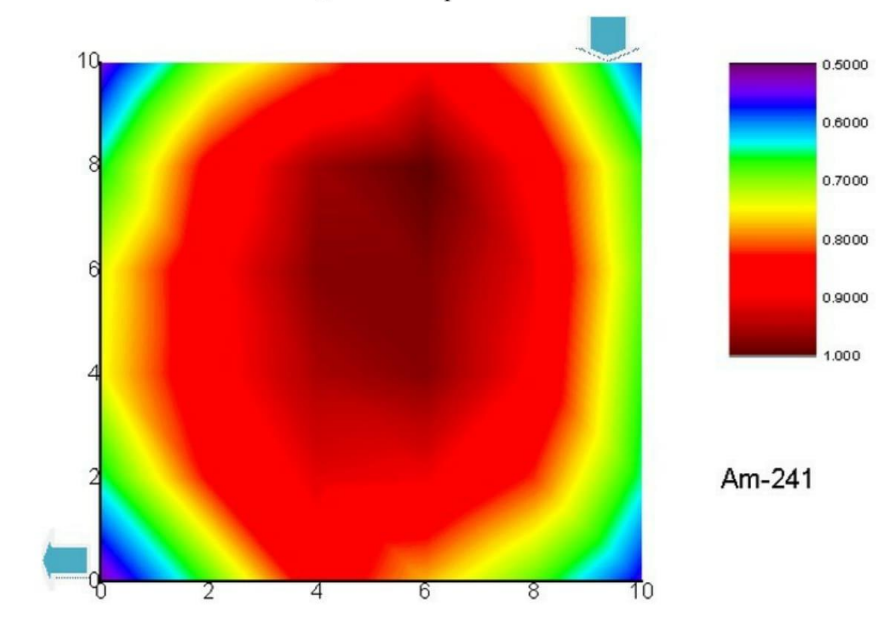


**Figure 9.** The figure shows the uniformity of the GEM prototype. Higher efficiencies are clearly shown at the center of the detector

## CONCLUSION

The GEM detector has become one of the most promising particle and radiation detectors nowadays. It has been utilized in various scientific researches including particle and nuclear physics, medical applications, astronomy, and national security. Since the  $10~\rm cm \times 10~\rm cm$  GEM prototype, which is designed by the GDD group at CERN, has simple designs and assemble procedures while still maintaining excellent properties, it is exceptionally suitable for both startup and advanced researches. Many researchers have relied their researches to the excellences in properties of the GEM prototype. This article reports the investigations on main properties of the GEM prototype, which include

- Plateau: the GEM prototype reached full efficiency when the power supply voltages reached 4100 V and became relatively constant when the voltages were greater than 4100 V.
- Gain: gains of the GEM prototype increased exponentially with the increase in power supply voltages. The relationship between gains and voltages could be described by the equation  $G=2\times 10^{-9}e^{0.0072V}$ .
- Signal sharing: it was found that X strips, which are narrower and located on the top layer of the readout, collected larger signals than Y strips by ~30%.
- Uniformity: the GEM prototype had higher efficiencies at the center of the active area, while areas near edges had lower efficiencies.

These investigations are very useful for researchers to use as future references and to better understand behaviors of the GEM detector. Further researches on the GEM detector should be followed in order to improve and to widen possible applications.

## ACKNOWLEDGEMENT

We gratefully acknowledge a financial support from the Faculty of Science and Kasetsart University the grant no. RFG2-5.

# REFERENCES

- 1. F. Sauli, "A new concept for electron amplification in gas detectors", *Nucl. Instr. and Meth. A.*, **1997**, 386, 531.
- GDD. "Performances of GEM detectors", http://gdd.web.cern.ch/GDD/. (Accessed: June 2015).
- 3. R. Wang, "A practical method to determine the spatial resolution of GEM detector", *Nucl. Instr. and Meth. A.* **2012**, 701, 54-57.
- K. Gnanvo, N. Liyanage, V. Nelyubin, K. Saenboonruang, S. Sacher and B. Wojtsekhowski, "Large size GEM for Super Bigbite Spectrometer (SBS) polarimeter for Hall A 12 GeV program at JLab", Nucl. Instr. and Meth. A. 2015, 782, 77-86.
- M. Danielsson, P. Fonte, T. Francke, C. Iacobaeus, J. Ostling and V. Peskov, "Novel gaseous detectors for medical imaging", *Nucl. Instr. and Meth. A.* 2004, 518, 406-410.
- H. Andersson, et al., "Gem detectors for X-ray astronomy", Nucl. Instr. and Meth. A. 2003, 513, 155-158.
- 7. H. Ohshita, et al., "Development of a neutron detector with a GEM", *Nucl. Instr. and Meth. A.* **2010**, 623, 126-128.
- K. Saenboonruang, "Recent developments in GEM-based neutron detectors" *Journal of Physics: Conference Series*, 2015, 611, 012016.
- Cremat, "CR-110 charge sensitive preamplifier: application guide", 2014, http://www.cremat.com/CR-110.pdf. (Accessed: June 2015).
- 10. M. Zecchin, "Characterization of a triple-GEM detector prototype for the CMS muon spectrometer upgrade with GEM detectors", *PhD thesis*, **2014**, Universitas Bruxellensis.

7.3 Manuscript entitle "Comparisons of GEM-Based Neutron Detectors with <sup>10</sup>B/<sup>nat</sup>B-coated Cathode and Ar/CO<sub>2</sub> (He/CO<sub>2</sub>) Gas Flow", which is under review for publication on "Chiang Mai Journal of Science"

Comparisons of GEM-Based Neutron Detectors with <sup>10</sup>B/<sup>nat</sup>B-coated Cathode and Ar/CO<sub>2</sub> (He/CO<sub>2</sub>) Gas Flow

Kiadtisak Saenboonruang \*[a], Piyakul Kumpiranon [a], Jatechan Channuie [b] and Thiraphat Vilaithong [c]

- [a] Department of Applied Radiation and types, Faculty of Science, Kasetsart University, Chatuchak, Bangkok, 10900, Thailand
- [b] Nuclear Research and Development Division, Thailand Institute of Nuclear Technology, Ongkharak, Nakhon Nayok, 26120, Thailand
- [c] Thailand Center of Excellence in Physics, CHE, Bangkok, 10400, Thailand

\*Author for correspondence; e-mail: fscikssa@ku.ac.th

#### **ABSTRACT**

Since its invention in 1997, the Gas Electron Multiplier (GEM) detector has been utilized in various applications including high-precision tracking devices in nuclear and particle physics researches. Typically, the standard GEM detector is suitable for ionizing particle detection, however, by introducing neutron converters to GEM, it could also be used as a neutron detector. This article reports properties of the GEM-based neutron detector using different thicknesses and types of boron (10 and 10 and 10 and 10 coated on the GEM cathode with either Ar/CO<sub>2</sub> (70:30) or 4He/CO<sub>2</sub> (80:20) gas flow. Two main properties: relative efficiencies and gains, are carefully investigated. Results show that the modified GEM detector is able to detect both thermal and fast neutrons with different characteristics depending on thicknesses and types of boron, types of gas flow, and voltages supplied to the GEM detector. Introduction to GEM detectors, materials used, testing procedures, and results are discussed in this article.

Keywords: neutron, thermal neutron, fast neutron, boron, helium, GEM detector

## 1. INTRODUCTION

Requirements for present detection methods have commanded us to go beyond our current capabilities. More advanced knowledge and technologies are investigated in order to overcome all limitations. In particular, techniques to detect ionizing particles and radiations have become important tools in many scientific researches to understand all phenomena: from minuscule quarks to a vast universe. The gas electron multiplier (GEM) detector was first invented by F. Sauli and his associates in 19971 [1] and has become one of the most promising particle detectors nowadays. Due to GEM's excellences in spatial resolution (~ 50 µm) [2], higher rates of detection capabilities (exceeding 10<sup>5</sup> Hz/mm²) [3], flexibility in designs, and relatively lower cost of manufacture, it meets the needs for a number of highly-rated nuclear and particle experiments including COMPASS [4], TOTEM [5],  $G^p_E$ ,  $G^n_M$  [6]. Furthermore, the GEM detector is also recommended for high-precision tracking devices for future PREX-like experiments that require high rates of detection [7].

Main components of a standard GEM detector consist of:

- GEM cathode: a framed aluminized polyimide (Kapton) placed topmost of the stack inside the GEM chamber. The most negative voltage is supplied to the cathode on the aluminum side such that electrons produced during ionizations would drift toward GEM foils;
- GEM foils: thin multilayer foils used in electron amplification stages. Each GEM foil consists of a 50-μm polyimide foil sandwiched by two thin copper plates. GEM foils are perforated [8] to have arrays of 70-μm holes called GEM holes. Each GEM hole is 140 μm apart from its adjacent GEM holes. Voltage differences of 300-450 V are supplied between two thin copper plates such that strong electric fields are created inside these GEM holes. Once groups of primary electrons drifting from a GEM cathode accelerate toward the first GEM foil, they would acquire higher kinetic energy and be able to further ionize gas molecules inside the detector. These processes would produce large groups of electron

- avalanches. Two or three GEM foils are usually cascaded in order to amplify numbers of electrons to be large enough for detection;
- GEM readout: pads or strips that are able to collect and transfer electron
  avalanches at the end of the amplification stage to an appropriate data acquisition
  (DAQ) system for data processing. For a standard GEM detector, a common
  layout consists of two sets of thin wires running perpendicular to each other in X
  and Y directions.

In addition to the three components mentioned above, the GEM detector also has inlets and outlets for proper gas to flow through. Types of gas used vary depending on applications, however, a gas mixture of Ar/CO<sub>2</sub> (70:30), where CO<sub>2</sub> acts as a quenching gas, is suitable for most applications.

In a normal configuration, the GEM detector is suitable for low-energy photons and ionizing particles detection such as x-rays, betas, and alphas. However, by inserting appropriate neutron converters to the detector, the GEM detector could also be used to detect neutrons. Since fast neutrons and thermal neutrons interact differently with different types of neutron converters, performances in the detection strongly depend on choices of neutron converters. This article aims to characterize a GEM detector with different converters to detect thermal and fast neutrons.

# 1.1 THERMAL NEUTRON DETECTION

A thermal neutron is a free neutron that has kinetic energy of 0.025 eV, which is the most probable velocity of neutrons at room temperature. Since neutrons are electrically neutral, they are unable to directly ionize gas molecules inside the GEM detector the same way as charged particles do. Hence, a mechanism that converts thermal neutrons to other ionizing particles is crucial for neutron detection. To serve the needs for thermal neutron conversion, a nuclear reaction between thermal neutrons and high-neutron-absorption-cross-section materials such as <sup>3</sup>He, <sup>6</sup>Li, or <sup>10</sup>B could be used [9]. In the past, most neutron detectors used <sup>3</sup>He as a thermal neutron converter due to its relatively high neutron

absorption cross section ( $\sigma_{abs}$ ) until there was a severe shortage of <sup>3</sup>He supply, leading to concerns of inadequate <sup>3</sup>He-based neutron detectors for many applications including national security, medical imaging, and scientific researches [10]. Several attempts were made to ease the problem. One possible and efficient solution is to replace <sup>3</sup>He with an alternative high-neutron-cross-section material such as <sup>10</sup>B. Although  $\sigma_{abs}$  of <sup>10</sup>B is lower than <sup>3</sup>He, <sup>10</sup>B is more abundant and less expensive. A mechanism of a nuclear interaction between <sup>10</sup>B and a thermal neutron, i.e. <sup>10</sup> B(n, $\alpha$ )<sup>7</sup>Li, is shown in Fig. 1a.

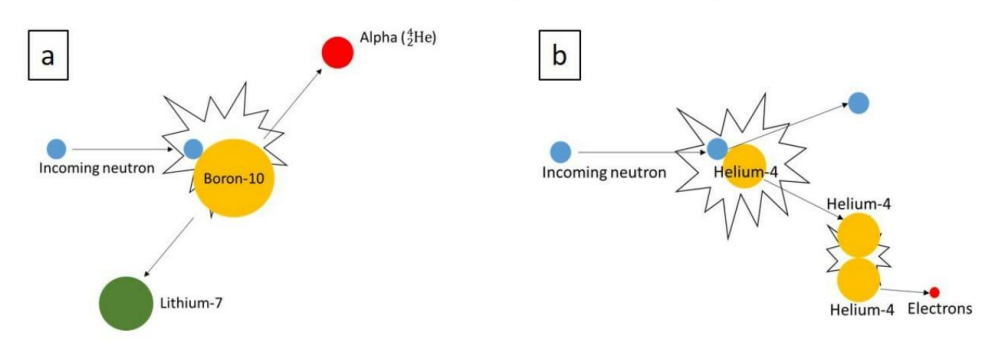


Figure 1: [a] The mechanism of a nuclear interaction between a thermal neutron and <sup>10</sup>B, which produces <sup>7</sup>Li and a 1.47-MeV alpha traveling in opposite directions and [b] the mechanism of an elastic scattering of a fast neutron off <sup>4</sup>He nucleus.

Another interesting choice for  $^{3}$ He replacement is natural boron ( $^{nat}$ B), which consists of 19.9%  $^{10}$ B and 80.1%  $^{11}$ B. The mixture between the two isotopes subsequently decreases  $\sigma_{abs}$  of  $^{nat}$ B to  $\sim$ 763.3 barns. Despite the fact that the decrease in  $\sigma_{abs}$  of  $^{nat}$ B leads to less efficiency in neutron detection,  $^{nat}$ B is still an interesting choice to be considered as a neutron converter due to its much lower cost and simpler purification procedures compared to  $^{10}$ B, which requires isotope separation techniques [11].

To introduce either <sup>10</sup>B or <sup>nat</sup>B into a GEM detector, thin boron film is coated on the GEM cathode. Schematic drawing of the GEM-based neutron detector and its neutron converting processes are shown in Fig. 2. Since the efficiency of the GEM-based neutron

detector depends largely on the numbers of the interactions between thermal neutrons and boron nuclei, greater numbers of boron nuclei per unit area, which is directly proportional to boron film's thickness, could increase chances of the interaction and improve detector's efficiency. However, a 1.47-MeV alpha created during the conversion has very short ranges in boron film (~3.53 μm) as shown in Fig. 3. Thus, too thick boron film could adversely reduce numbers of alphas that penetrate through boron film and cause ionizations, leading to lower efficiency. To understand effects of types and thicknesses of boron film as a neutron converter, different thicknesses of <sup>10</sup>B and <sup>nat</sup>B were coated on cathodes to investigate efficiencies and gains of the GEM-based thermal neutron detector.

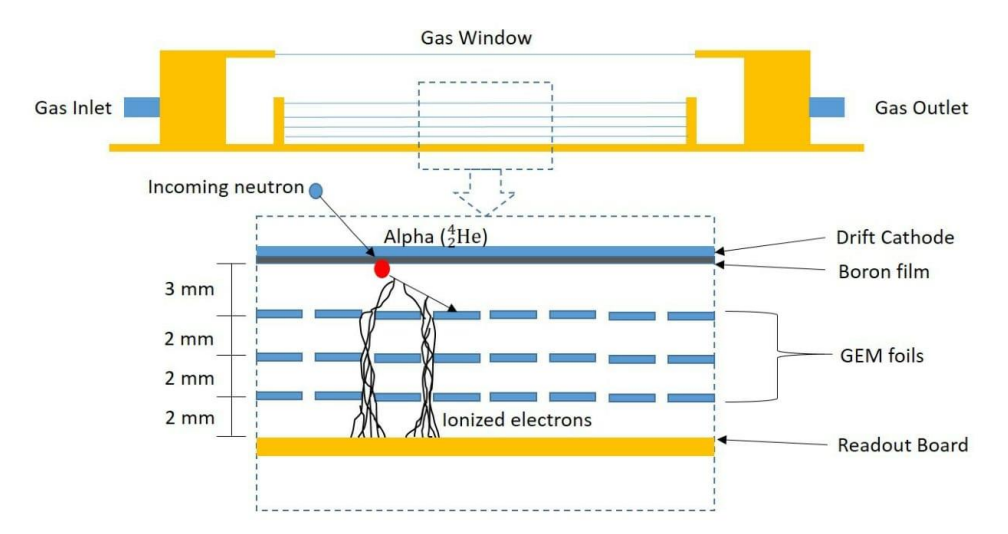


Figure 2: Schematic drawing of the GEM-based neutron detector and its neutron converting processes.

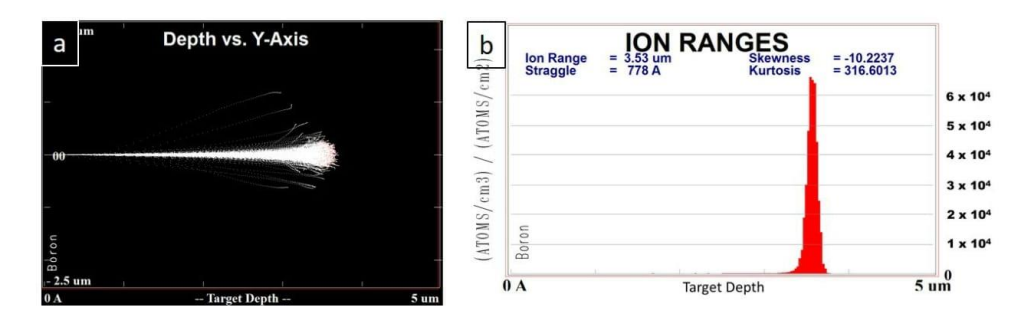


Figure 3: [a] the simulation of paths of 1.47-MeV alphas traveling through boron film and [b] the histogram of ranges of 1.47-MeV alphas travelling through boron film. The result was produced using SRIM-2013 program [12].

#### 1.2. FAST NEUTRON DETECTION

With its kinetic energy greater than 1 MeV, a fast neutron has higher kinetic energy than a thermal neutron. Since a fast neutron has extremely low chances of interaction with a neutron converter via nuclear reaction, the detection of a fast neutron relies on an elastic scattering of a fast neutron off light nuclei such as hydrogen nuclei or helium nuclei. The collisions between a fast neutron with another nucleus would cause a transfer of kinetic energy from the incoming fast neutron to recoil nuclei such that these recoil nuclei could ionize gas molecules for detection.

For a nucleus of atomic weight, *A*, the maximum energy transferred from an incoming neutron having energy, *E*, to a recoil nucleus is [13]:

$$E_{max} = \frac{4AE}{(A+1)^2} \tag{1}$$

From Eq. 1, it is clear that light nuclei would be a better choice than heavier nuclei to be used as a fast neutron converter as significant energies are transferred to the recoil nuclei, thus, higher chances of ionizing gas molecules. In principle, <sup>1</sup>H would be the most probable choice, however, pure H<sub>2</sub> or hydrogen-contained gas are usually flammable and could possibly cause damages to the detector. An alternative and reasonable choice of <sup>1</sup>H would be <sup>4</sup>He. Although the energy transferred from a fast neutron to <sup>4</sup>He nuclei is smaller <sup>1</sup>H

nuclei, <sup>4</sup>He nuclei are inert and nonflammable, thus safer to the detector. The mechanism of an elastic scattering of a fast neutron off a <sup>4</sup>He nucleus and a process in which the recoil nucleus ionizes other <sup>4</sup>He nucleus is shown in Fig. 1b.

#### 2. MATERIALS AND METHODS

#### 2.1. CONSTRUCTION AND INITIAL FUNCTIONALITY TESTS

A complete set of a 10×10 cm² triple-GEM detector was ordered from the Gas Detectors Development Group at CERN [14]. After receiving all components and completing preliminary tests such as current leakage of all GEM foils, the GEM detector were put together and performed initial tests including gas leakage test, discharged test, and preliminary x-ray detection test using 5.9-keV x-rays from <sup>55</sup>Fe. A gas mixture of Ar/CO<sub>2</sub> (70:30) was flowed through the detector with a constant flow rate of 3.0 L/hr during which a high voltage of -4,100 V was supplied to the GEM detector via a voltage divider circuit shown in Fig. 5. The precise gas flow rate was measured by a direct-reading flowmeter (Cole-Parmer Model 3204776) and was adjusted from times to times to ensure steady flow rates throughout the measurement. Since the measurement only records counts of detection and average signal amplitudes, the readout strips were combined into one connector and connected to a preamplifier (Canberra Model 2006), an amplifier (Ortec Model 590A), an oscilloscope, and a counter and timer (Canberra Model 2071A) for data acquisition. The equipment setup for initial tests and neutron tests is shown in Fig. 6.

After completing all initial tests, 99.9% <sup>10</sup>B was coated onto the cathode using Tribo-Kote S-X1 technique performed by Richter Precision, Inc. [15] However, the manufacturer was only able to coat the cathode with 1-μm thick of <sup>10</sup>B. The picture of a comparison between <sup>10</sup>B-coated cathode and a normal cathode is shown in Fig. 4. In the case of <sup>nat</sup>B, it was coated onto the cathode using an electron beam evaporation technique [16] performed at the National Electronics and Computer Technology Center (NECTEC), Thailand. The coated thicknesses of <sup>nat</sup>B were 2.5, 3.5, and 4.5 μm. Cathodes with <sup>nat</sup>B coating thicker than 4.5 μm have shown some cracks along the film surface and could not be used effectively.



Figure 4: A comparison of a cathode coated by a 1-μm 10 B (left) and a normal cathode (right).

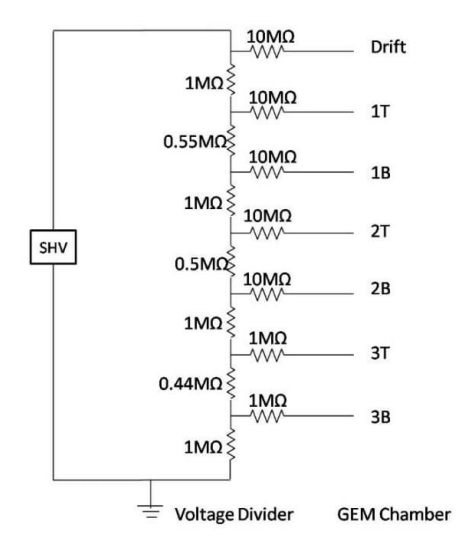


Figure 5: The voltage divider circuit used to supply high voltage to the GEM detector.

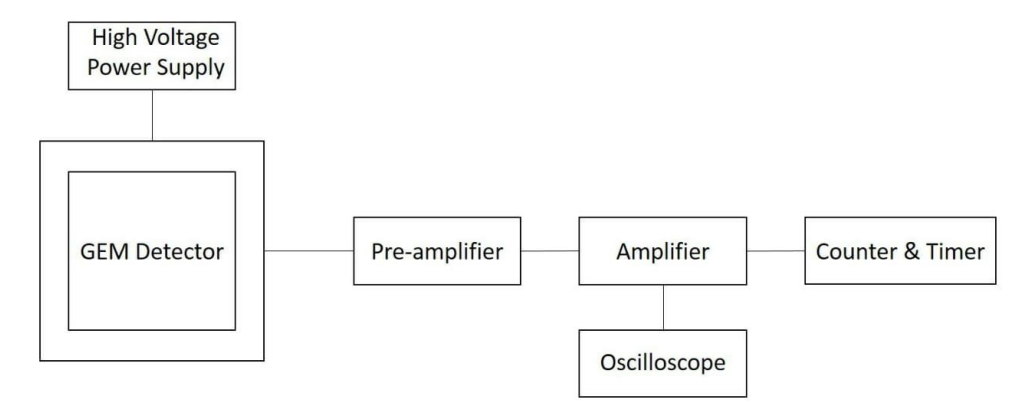


Figure 6: A schematic setup of the GEM detector during the measurement.

#### 2.2. THERMAL AND FAST NEUTRON TESTS

Following the initial tests to ensure functionality of the GEM detector, the normal cathode was replaced by a 1-µm <sup>10</sup>B-coated cathode. The detector was then moved to a test station. The layout of the test station is shown in Fig. 7a.

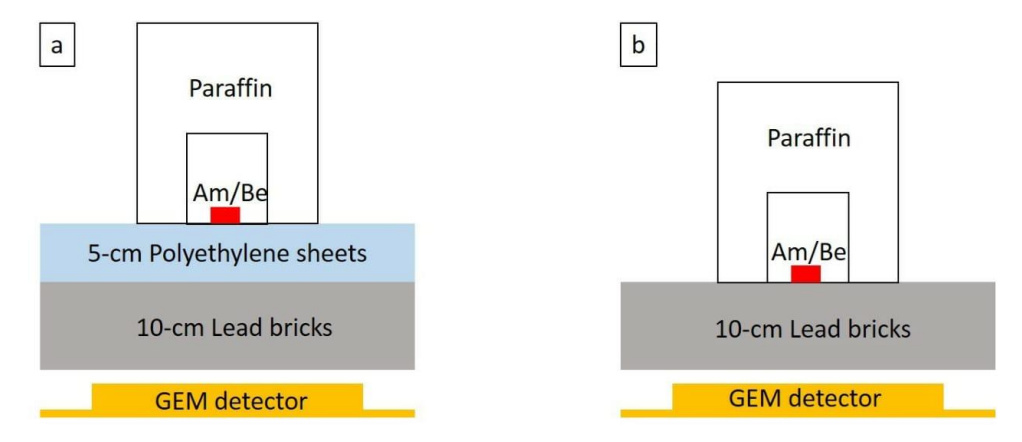


Figure 7: A schematic setup of the GEM detector for [a] thermal neutron detection and [b] fast neutron detection.

The 5-cm polyethylene (PE) sheets were used to thermalize fast neutrons from a 300-mCi <sup>241</sup>Am/Be source, while 10-cm lead bricks were used to shield gamma. The thickness of PE sheets was optimized at 5 cm for the highest yield of thermal neutrons measured using a <sup>3</sup>He neutron detector. Also, to ensure the least counts of gamma

contributed to neutron counts, a gamma-sensitive Geiger counter was used to measure backgrounds in two cases: with and without 241Am/Be above the detector. Results showed that no significant differences between two cases were observed. Thus 10-cm lead bricks were sufficient for gamma shielding. A gas mixture of Ar/CO<sub>2</sub> (70:30) was first flowed through the GEM detector to measure count rates (relative efficiencies) and signal amplitudes (relative gains), while varying voltages from -3,900 up to -4,400 V in 50-V increments. To determine the average thermal neutron count rate and signal amplitude for each voltage, 10 sets of 5 minutes long measurement were performed. Counts and amplitudes of signals larger than threshold level (0.035 A.U.) were used to find average values. After completing all necessary thermal neutron tests, the 5-cm PE sheets were removed so that fast neutrons could pass through the GEM detector without getting thermalized (Fig. 7b). All required measurement procedures were repeated for fast neutron detection, however, the duration for each set of measurement was extended to 50 minutes long due to its much lower count rates. For both thermal and fast neutron tests, background counts (without a neutron source presented) were measured and properly subtracted from the values with neutron source. Next, the gas mixture was switched to <sup>4</sup>He/CO<sub>2</sub> (80:20) and the 5-cm PE sheets were inserted back in place to thermalize fast neutrons. The procedures were then repeated as in the case of Ar/CO2 for both thermal and fast neutron tests. However, the threshold level for <sup>4</sup>He/CO<sub>2</sub> was raised to 0.1 A.U. due to higher noises during the measurement.

After completing all required measurement for a 1-µm <sup>10</sup>B-coated cathode, the cathode was replaced by a 2.5, 3.5, and 4.5-µm <sup>nat</sup>B coated cathodes respectively and all above procedures were repeated for both thermal and fast neutron measurements. A diagram of the experimental flow chart is shown in Fig. 8.

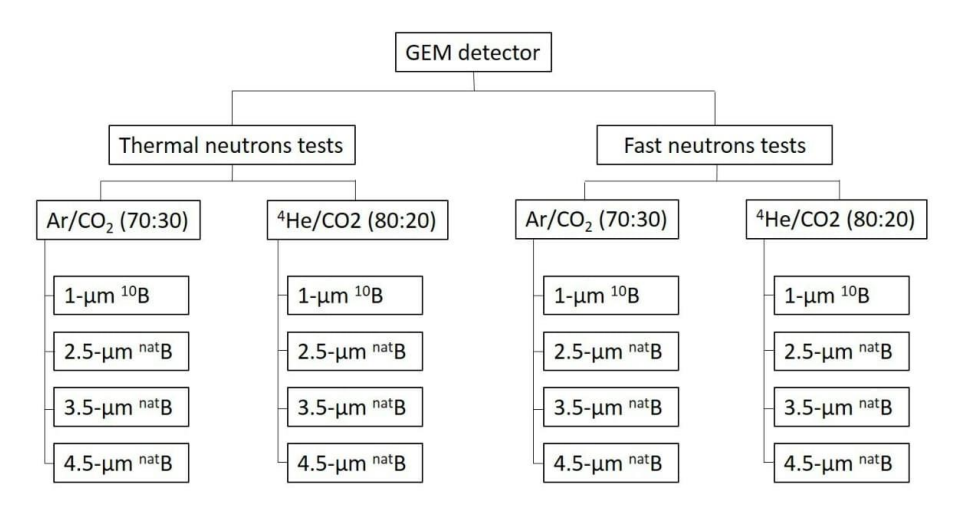


Figure 8: Experimental flow chart for GEM-based neutron detector.

## 3. RESULTS AND DISCUSSION

## 3.1 THERMAL NEUTRON DETECTION

For thermal neutron tests, 1-μm <sup>10</sup>B and 2.5, 3.5, 4.5-μm <sup>nat</sup>B-coated cathodes were used as neutron converters with either Ar/CO<sub>2</sub> (70:30) or <sup>4</sup>He/CO<sub>2</sub> (80:20) flowing through the detector. Results of count rates (counts/minute), which represent relative efficiencies, and signal amplitudes, which represent relative gains of the detector, for each combination are shown in Fig. 9 and Fig. 10 respectively.

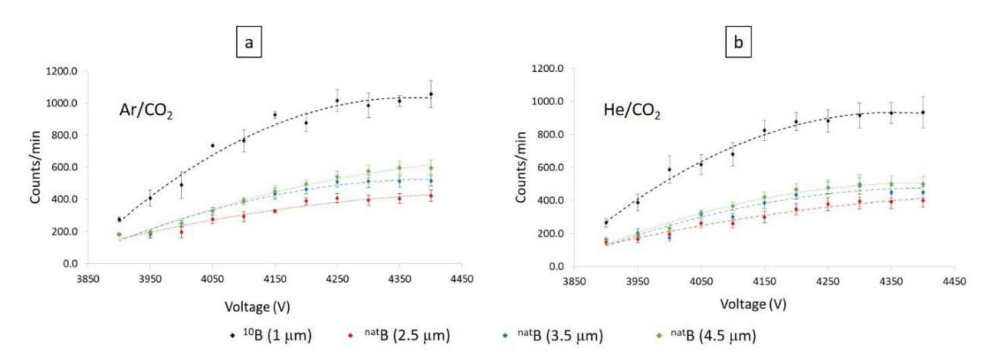


Figure 9: Plots showing relationship between thermal neutron count rates (counts/minute) and voltages supplied to the detector using gas mixtures of [a] Ar/CO<sub>2</sub> (70:30) and [b] He/CO<sub>2</sub> (80:20).

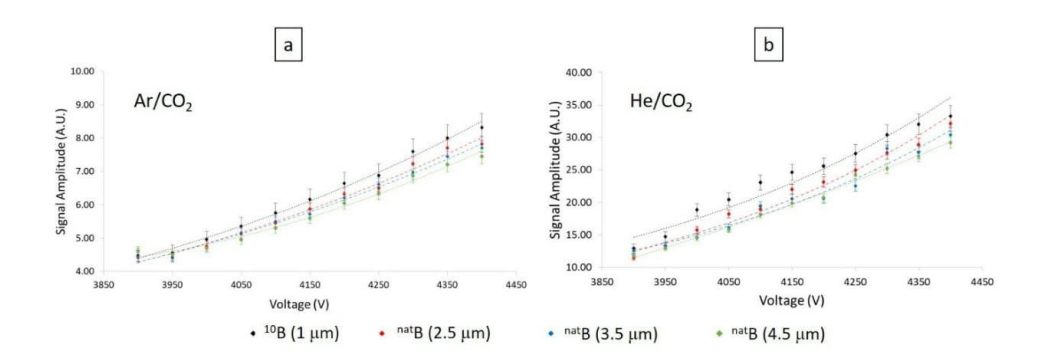


Figure 10: Plots showing relationship between signal amplitudes in thermal neutron detection and voltages supplied to the detector using gas mixtures of [a] Ar/CO<sub>2</sub> (70:30) and [b] He/CO<sub>2</sub> (80:20).

Fig. 9 shows that, for both types of gas, thermal neutron count rates increased as voltage supplied increased and reached plateau when the voltage was approximately -4,200 V. Also, the setup, which the cathode was coated by 1-μm <sup>10</sup>B, had the highest count rates compared to any other thickness of <sup>nat</sup>B. This is because, despite only 1 μm thick, <sup>10</sup>B has the value of neutron absorption cross section approximately 5 times higher than <sup>nat</sup>B, leading to more interactions between thermal neutrons and boron nuclei. However, as thicknesses of <sup>nat</sup>B increased, the count rates of detection also increased as more <sup>nat</sup>B nuclei were available for interactions. Fig. 10 shows that, for both types of gas mixtures, signal amplitudes increased as voltage supplied increased. The increase in the amplitudes was caused by stronger electric fields inside GEM holes, hence, resulted in more ability to amplify electrons.

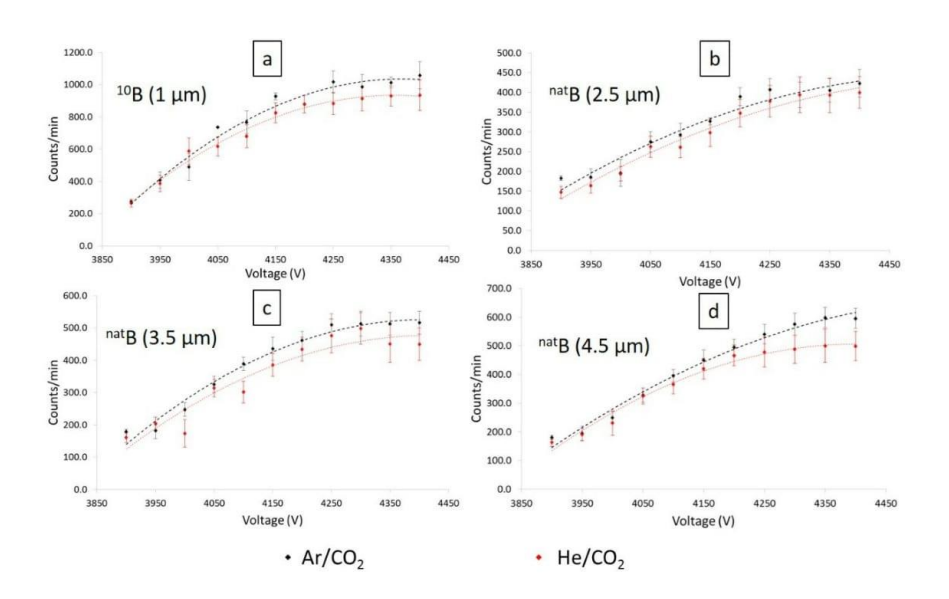


Figure 11: Plots showing relationship between thermal neutron count rates (counts/minute) and voltages supplied to the detector for cathodes coated by [a] 1 μm of <sup>10</sup>B, [b] 2.5 μm of <sup>nat</sup>B, [c] 3.5 μm of <sup>nat</sup>B, and [d] 4.5 μm of <sup>nat</sup>B.

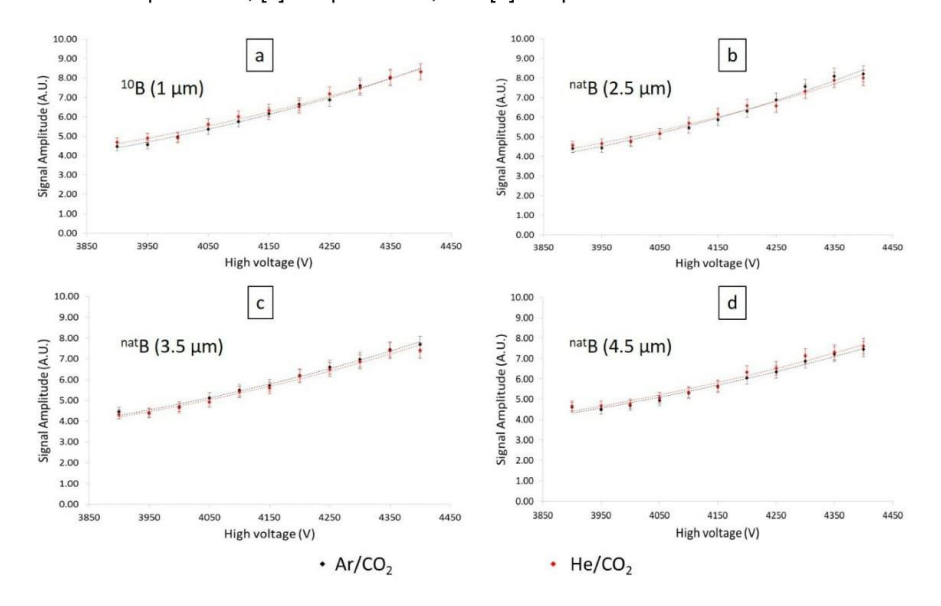


Figure 12: Plots showing relationship between signal amplitudes in thermal neutron detection and voltages supplied to the detector for cathodes coated by [a] 1  $\mu$ m of <sup>10</sup>B, [b] 2.5  $\mu$ m of <sup>nat</sup>B, [c] 3.5  $\mu$ m of <sup>nat</sup>B, and [d] 4.5  $\mu$ m of <sup>nat</sup>B.

As shown in Fig. 11, the setup that had Ar/CO<sub>2</sub> flowed through had slightly higher count rates than the one with <sup>4</sup>He/CO<sub>2</sub> for all types/thicknesses of boron coating. This is because the setup with <sup>4</sup>He/CO<sub>2</sub> was less stable and had about three times higher in electronic background levels compared to Ar/CO<sub>2</sub>. These characteristics eliminated some signals that were large enough in the case of Ar/CO<sub>2</sub> but too small for <sup>4</sup>He/CO<sub>2</sub>. However, as shown in Fig. 12, signal amplitudes for <sup>4</sup>He/CO<sub>2</sub> were approximately the same as Ar/CO<sub>2</sub> for all types/thicknesses of boron coating. The result was a bit unexpected as a <sup>4</sup>He nucleus has higher minimum ionization energy than an argon nucleus, which should create less primary electrons and smaller signal amplitude. However, due to higher threshold values of <sup>4</sup>He/CO<sub>2</sub>, smaller-than-threshold signals were not detected and used to find average signal amplitudes in the case of <sup>4</sup>He/CO<sub>2</sub>.

## 3.2 FAST NEUTRON DETECTION

For fast neutron detection, the setup with a gas mixture of Ar/CO<sub>2</sub> did not show enough statistic count rates after background subtracted because energies transferred from fast neutrons to argon nuclei are too small (Eq. 1) for recoil nuclei to cause further ionizations. On the other hand, in the setup with <sup>4</sup>He/CO<sub>2</sub>, higher energy could be transferred to <sup>4</sup>He nuclei and fractions of incoming fast neutrons could be detected even though its count rates were approximately ~100 times smaller than those of thermal neutrons due to less probability of ionizations. Results of fast neutron detection for of <sup>4</sup>He/CO<sub>2</sub> are shown in Fig. 13 and Fig. 14.

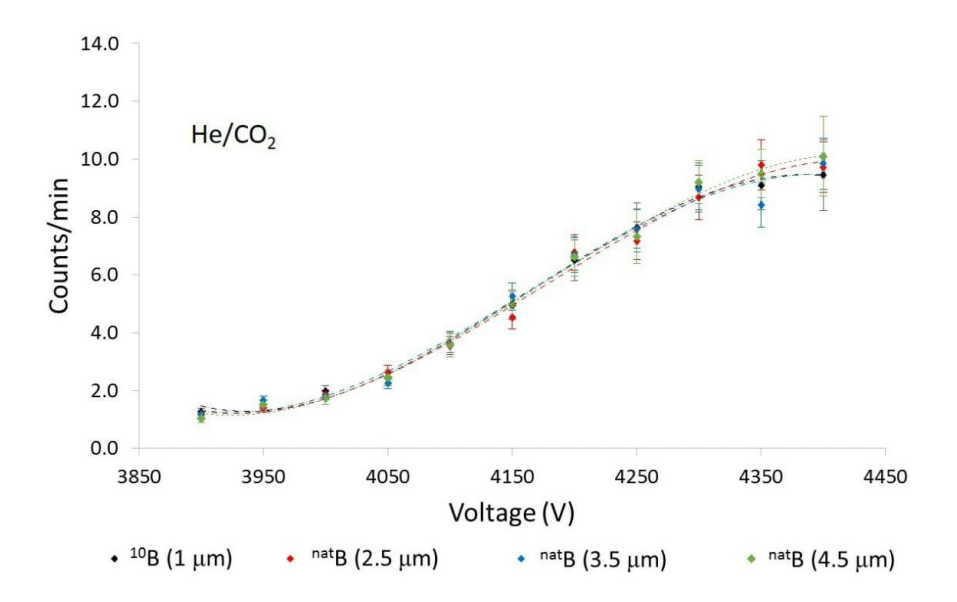


Figure 13: Plots showing relationship between fast neutron count rates (counts/minute) and voltages supplied to the detector for <sup>4</sup>He/CO<sub>2</sub> and cathodes coated by different types/thicknesses of boron.

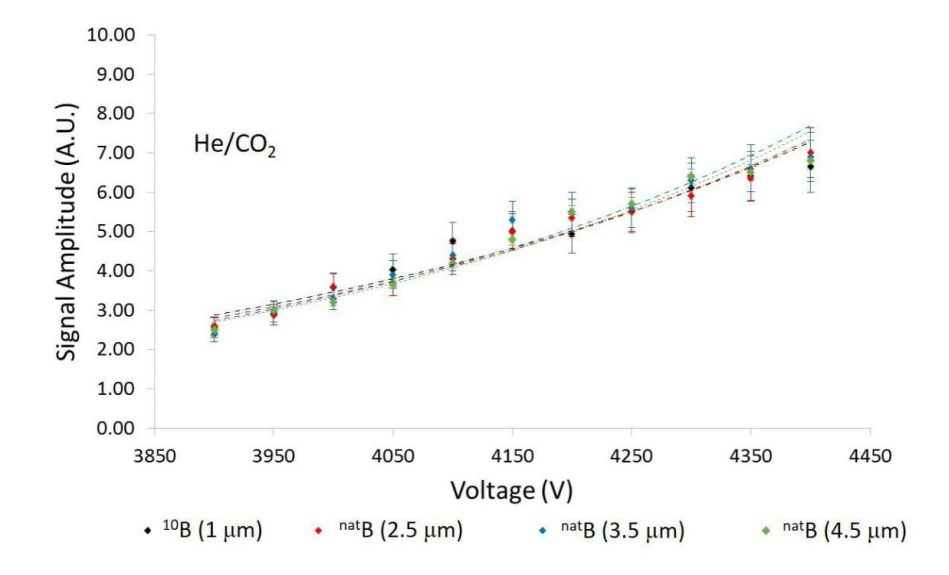


Figure 14: Plot showing relationship between signal amplitudes in fast neutron detection and voltages supplied to the detector for <sup>4</sup>He/CO<sub>2</sub> and cathodes coated by different types/thicknesses of boron.

As shown in Fig. 13 and Fig. 14, count rates and signal amplitudes increased as voltage supplied increased and reached plateau when the voltage was approximately -4,250 V. Furthermore, results showed that count rates and signal amplitudes for different types/thicknesses of boron did not have effects on the detector's performances for fast neutron detection since boron nuclei have little or no significant nuclear interactions with fast neutrons.

#### 4. CONCLUSIONS

In addition to the ability to detect ionizing particles, the Gas Electron Multiplier (GEM) detector could also be used as both thermal and fast neutron detectors. The performance in the detection depends on types of neutron converters applied to the detector, leading to different detection mechanisms. Detection of thermal neutrons relies on nuclear interactions between thermal neutrons and nuclei of neutron converters, which in this research, were either <sup>10</sup>B or <sup>nat</sup>B. The GEM with its cathode coated by 1-µm <sup>10</sup>B had the highest detection count rates, despite its thinnest coating compared to <sup>nat</sup>B. However, as thickness of <sup>nat</sup>B coating increased, the GEM could detect thermal neutrons with higher efficiencies. In the case of fast neutrons, the detection relies on elastic scattering of fast neutrons off light nuclei such as <sup>4</sup>He nuclei. Although the efficiency of fast neutron detection was much less than thermal neutron detection, results showed that, by changing types of gas flow from a usual Ar/CO<sub>2</sub> to <sup>4</sup>He/CO<sub>2</sub> without any other modification to the normal GEM detector, the detector could be used to detect fast neutrons. These results do not only show capabilities of the GEM detector to detect neutrons but also present ideas and references for researchers to select suitable neutron converters for different applications.

## 5. ACKNOWLEDGEMENT

This work was supported by The Thailand Research Fund (TRF) under Grant No. TRG5780292; Kasetsart University, and Faculty of Science under Grant No. RFG2-5. We would also like to acknowledge supports from Kasetsart University Research and

Development Institute (KURDI), Department of Applied Radiation and Isotopes, Thailand Institute of Nuclear Technology (TINT), and the National Electronics and Computer Technology Center (NECTEC), Thailand.

#### References

- [1] Sauli F., Nucl. Instr. and Meth. A. 1997; 386: 531-534.
- [2] Wang R., Huang Y., Xiao Z., Zhang Z., Wang R. and Gao H., Nucl. Instr. and Meth. A. 2013; 701: 54-57.
- [3] Bachmann S., Kappler S., Ketzer B., Muller T., Ropelewski L., Sauli F. and Schulte E., Nucl. Instr. and Meth. A. 2002; 478: 104-108.
- [4] Altunbas C., Capans M., Dehmelt K., Ehlers J., Friedrich J., Konorov I., Gandi A., Kappler S., Ketzer B., Oliveira R.D., Paul S., Placci A., Ropelewski L., Sauli F., Simon F. and Stenis M.V., Nucl. Instr. and Meth. A. 2002; 490: 177-203.
- [5] Quinto M., Berretti M., David E., Garcia F., Greco V., Heino J., Hilden T., Kurvinen K., Lami S., Latino G., Lauhakangas R., Oliveri E., Ropelewski L., Scribano A., Turini N. and Stenis M.V., Nucl. Phys. B (Proc. Suppl.). 2011; 215: 225-227.
- [6] Gnanvo K., Liyanage N., Nelyubin V., Saenboonruang K. Sacher S. and Wojtsekhowski B., Nucl. Instr. and Meth. A. 2015; 782: 77-86.
- [7] Saenboonruang K. and Liyanage N., Kasetsart J. (Nat. Sci.). 2015; 49: 277-287.
- [8] Chowdhury A. and Masud M., Gem: A comparison of single & double mask gems;
  Available at: <a href="http://www.academia.edu/1691839/Gas\_Electron\_Multiplier\_">http://www.academia.edu/1691839/Gas\_Electron\_Multiplier\_</a>
  GEM\_A\_comparison\_of\_single\_and\_double\_mask\_GEMs. Accessed: 2016-06-04.
- [9] Sears V.F., Neutron News. 1992; 3: 26-37.
- [10] Shea D. A. and Morgan A. The Helium-3 shortage: Supply, Demand, and Options for congress; Available from: https://www.fas.org/sgp/crs/misc/R41419.pdf/. Accessed: 2016-06-01.

- [11] Ragheb M., Isotopic separation and enrichment; Available from: http://mragheb.com/NPRE%20402%20ME%20405%20Nuclear%20Power %20Engineering/Isotopic%20Separation% Accessed: 2016-06-01.
- [12] Ziegler J. F., Interactions of ions with matter; Available from: http://www.srim.org/. Accessed: 2016-06-01.
- [13] Crane T. and Baker M. P. Neutron detector; Available from: http://www.lanl.gov/orgs/n/n1/panda/00326408.pdf/. Accessed: 2016-06-03.
- [14] GDD. How to get GEMs; Available from: http://gdd.web.cern.ch/GDD/. Accessed: 2016-06-04.
- [15] Richter Precision. PVD, CVD, TD & DCD Coatings; Available from: http://www.richterprecision.com/index.html/. Accessed: 2016-06-04.
- [16] Satou M. and Fujimoto F., Jpn. J. Appl. Phys. 1983; 22 (3) L171.

7.4 Manuscript entitled "Comparison of a GEM-based Fast Neutron Detector Using  $^4\text{He/CO}_2$  and  $^4\text{He/CO}_2$ /C $_4\text{H}_{10}$  Gas Mixtures", which is currently under review for publication on "Kuwait Journal of Science".

1

Comparison of a GEM-based Fast Neutron Detector Using  $^4He/CO_2$  and  $^4He/CO_2/C_4H_{10}$  Gas Mixtures

Kiadtisak Saenboonruang<sup>1\*</sup>, Piyakul Kumpiranon<sup>1</sup>, Khem Chirapatpimol<sup>2</sup>, Thiraphat Vilaithong<sup>3</sup>

<sup>1</sup>Department of Applied Radiation and Isotopes, Faculty of Science, Kasetsart University, Bangkok 10900, Thailand

<sup>2</sup>Department of Physics, Faculty of Science, Chiang Mai University, Chiang Mai, 50200, Thailand

<sup>3</sup>Thailand Center of Excellence in Physics, CHE, Bangkok, 10400, Thailand

Corresponding Author: Email: fscikssa@ku.ac.th

Abstract

<sup>1</sup>H- or <sup>4</sup>He-contained gas mixtures are usually used to detect fast neutron relying on elastic scattering between incoming fast neutrons and light gas molecules, due to their large energy transfer during collisions and higher chances of ionizations. In this research, gas mixtures of <sup>4</sup>He/CO<sub>2</sub> (80:20 and 70:30) and <sup>4</sup>He/CO<sub>2</sub>/C<sub>4</sub>H<sub>10</sub> (70:23:7) were flowed through a 10 cm×10 cm triple-Gas Electron Multiplier (GEM) detector at a constant flow rate of 3.0 L/hr in order to detect fast neutrons. Comparisons of relative efficiencies, relative gains, and detection uniformity for all gas types were investigated by measuring signal counts and signal amplitudes. Results showed that a gas mixture of <sup>4</sup>He/CO<sub>2</sub> (80:20) had the highest relative efficiency and relative gains amongst all gas mixture types. In terms of detection uniformity, detection efficiency at the center of the active area was approximately 20% higher than areas close to the detector edges. Details of basic knowledge of GEM, experimental procedures, results and discussion are included in this article.

Keywords: GEM detector; neutrons; fast neutrons; helium; efficiency

1. Introduction

1.1 Fast neutron detection

Fast neutrons, neutrons with energy greater than 1 MeV, are usually produced by nuclear processes such as in nuclear fissions, spontaneous fissions, nuclear fusions, and emissions from

61

neutron-rich nuclei. Since their discovery almost a century ago, knowledge and technology of fast neutrons have improved greatly, leading to utilizations in various applications including cargo scanning (Eberhardt *et al.*, 2005), airport security (Miller *et al.*, 1993), explosive detection (Gozani *et al.*, 2007), medical diagnostic (Laramore *et al.*, 1993), and radiotherapy (Douglas *et al.*, 2003; Bayanov *et al.*, 1998). Although different applications require different setups and equipment, common equipment is detectors with ability to detect either direct fast neutrons or energy-reduced (thermal) neutrons. The two main methods involving neutron detection are:

Elastic scattering of fast neutrons off light nuclei. This method relies on the energy
transfer from an incoming fast neutron to a light nucleus during their collision such that
the recoiled nucleus acquires enough energy to ionize gas molecules inside the detector
for detection. A process of the elastic scattering is shown in Fig. 1;

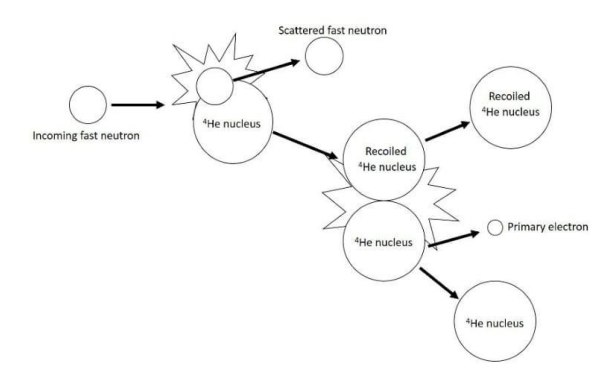


**Fig. 1.** Mechanism of an elastic scattering of a fast neutron off 4 He nucleus for fast neutron detection.

• Nuclear reaction between thermal neutrons and high-neutron-absorption-cross-section nuclei. To detect fast neutrons, this method requires hydrogen-rich materials such as water or high density polyethylene (HDPE) to thermalize (reduce energy of) fast neutrons to approximately 0.025 eV. Since thermal neutrons have high chances of interactions to produce secondary ionizing particles with some nuclei such as <sup>3</sup>He and <sup>10</sup>B via nuclear reactions, the detection of fast neutrons is typically done by converting fast neutrons to thermal neutrons and ionizing particles, which are subsequently detected.

Although both methods are able to detect neutrons, their detection properties are quite different. For example, detection through nuclear reactions has shown better detection efficiencies than detection through elastic scattering due to its larger neutron cross sections (Crane *et al.*, 1991). However, detection through nuclear reactions require varying degrees of modifications to detectors as moderators and neutron converters must be introduce or embedded to the detection system (Prasad *et al.*, 2000; Lacy *et al.*, 2011). On the other hand, elastic scattering method is relatively simpler to operate as the only additional procedure required is to switch types of gas flow through the detector to <sup>1</sup>H- or <sup>4</sup>He-contained gas mixtures, while other components remain the same.

#### 1.2 Gas Electron Multiplier (GEM) detector

A GEM detector is a gaseous particle detector that has been developed and used primarily in nuclear and particle researches for almost 20 years (Sauli, 1997; Gnanvo et al., 2015). In addition, due to their promising properties such as excellent spatial resolution (50 µm or better), high rate capability (10<sup>5</sup> Hz/mm<sup>2</sup>), flexibilities in designs, and relatively low cost, the GEM detector has been used in many other applications including medical imaging (Danielson et al., 2004), astrophysics (Anderson et al., 2003), and neutron detection (Ohshita et al., 2010). A standard triple-GEM detector consists of three GEM foils which are 50-um thin insulating polyimide foils. Each GEM foil is sandwiched by two thin copper plates. The GEM foil is perforated with arrays of 70-µm diameter GEM holes having 140-µm pitches between two adjacent holes. Two GEM foils are spaced 2 mm apart from each other. A voltage difference of 250-400 V is supplied to the two copper plates such that strong electric fields are formed inside GEM holes. On top of GEM foil stack is a drift cathode usually made of a thin sheet of aluminized polyimide where the aluminum side facing towards GEM foils is supplied with the most negative voltage (approximately -4000 V using the voltage divider shown in Fig. 2). All GEM foils and the drift cathode are enclosed in a gas-tight box with one gas inlet and one gas outlet. Readout of a standard GEM detector has an XY configuration with two sets of 256 thin conducting wires running perpendicular to each other in X and Y directions. An appropriate data acquisition (DAQ) system is connected to the readout for data processing. The schematic drawing of the standard triple-GEM detector is shown in Fig. 3.

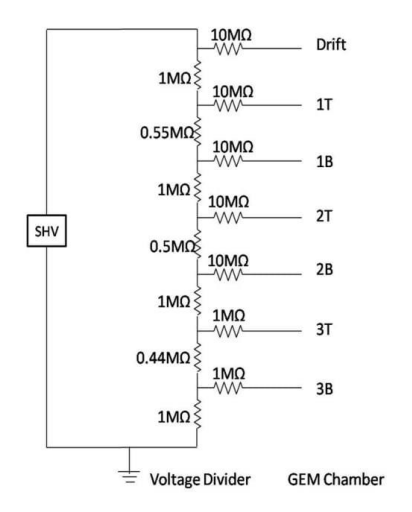
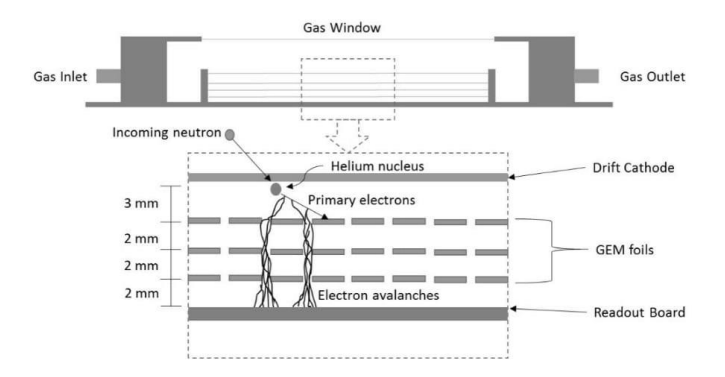


Fig. 2. A voltage divider circuit used to supply high voltage to the GEM detector during the tests.



**Fig. 3.** Schematic drawing of the standard triple GEM detector and the mechanism of fast neutron detection through an elastic scattering between an incoming fast neutron and a <sup>4</sup>He nucleus.

#### 1.3 GEM-based fast neutron detector

A GEM detector could be modified to detect fast neutrons. Many previous researches and applications have relied their detection ability through nuclear reactions using high neutron-absorption-cross-section neutron converters such as coating of the GEM drift cathode and GEM foils with a thin film of  $^{10}$ B. Numbers of results were reported and are widely available for references (Ohshita *et al.*, 2010; Saenboonruang, 2015). On the other hand, information on the detection of fast neutrons through an elastic scattering off light nuclei is inadequate and needs thorough investigations. In principle,  $^{1}$ H would be the most probable choice for fast neutron detection due to its highest energy transfer to recoiled nuclei during the collision as shown in Eq. 1, where  $E_{max}$  is the maximum energy that could be transferred from an incoming neutron to a target nucleus, A is the atomic weight of a target nucleus, and E is the energy of an incoming neutron.

$$E_{max} = \frac{4AE}{(A+1)^2} \tag{1}$$

However, pure H<sub>2</sub> or hydrogen-contained gas are flammable. Consequently, only a few percent of hydrogen-contained gas are allowed to operate in most gaseous detectors. An alternative and reasonable choice of <sup>1</sup>H would be <sup>4</sup>He. Although the energy transfer from a fast neutron to a 4He nucleus is smaller than in the case of <sup>1</sup>H, <sup>4</sup>He nuclei are inert and nonflammable, thus safer to the detector. The mechanism of an elastic scattering of a fast neutron off a <sup>4</sup>He nucleus and a process in which the recoiled nucleus ionize other <sup>4</sup>He nucleus is shown in Fig. 3. This article compares properties of a GEM-based fast neutron detector using three different gas mixtures: <sup>4</sup>He/CO<sub>2</sub> (80:20 and 70:30) and <sup>4</sup>He/CO<sub>2</sub>/C<sub>4</sub> H<sub>10</sub> (70:23:7) at a constant flow rate of 3.0 L/hr. The addition of 7% C<sub>4</sub>H<sub>10</sub> was intended to increase stability of the detection as reported in Bencivenni *et al.*, 2003 and Alfonsi *at al.*, 2004. Relative efficiencies, relative gains, and uniformity of the detector were investigated by measuring signal counts and signal amplitudes for each gas type.

## 2. Experiment

# 2.1 Construction and initial tests

Standard triple-GEM components with active area of 10 cm×10 cm were ordered from the Gas Detector Development Group at the European Organization for Nuclear Research (CERN). Current leakages from each GEM foil were carefully measured in a N<sub>2</sub> -filled sealed box to ensure its current amplitudes were smaller than 200 nA. All GEM components were put together in a class-1000 cleanroom and further tests including gas leaks, discharged frequencies, and preliminary 5.9-keV x-ray detection were performed. During the initial tests, a gas mixture of Ar/CO<sub>2</sub> (70:30) was flowed through the detector with a constant flow rate of 3.0 L/hr and a high voltage of -4100 V was supplied to the GEM detector via a voltage divider circuit shown in Fig. 2. The precise gas flow rate was measured by a direct-reading flow meter (Cole-Parmer Model 3204776) and was adjusted from times to times to ensure steady flow rates throughout the measurement. Since only signal counts and average signal amplitudes were recorded, the 256 readout strips on X side were combined into one connector and connected to a preamplifier (Canberra Model 2006), an amplifier (Ortec Model 590A), an oscilloscope (Hantek DSO 5202B), and a counter and timer (Canberra Model 2071A) for data acquisition. The equipment setup for initial tests and neutron tests is shown in Fig. 4.

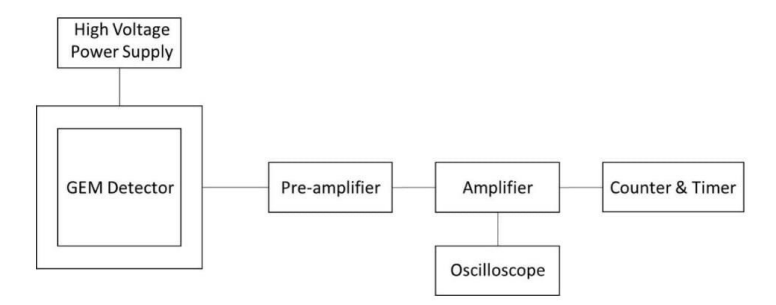
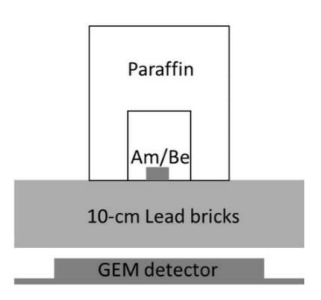


Fig. 4. Equipment setup for GEM's tests.

## 2.2 Fast neutron detection tests

After completing initial tests with satisfactory results, the gas flow was changed from  $Ar/CO_2$  (70:30) to  $^4He/CO_2$  (80:20 and 70:30) and  $^4He/CO_2/C_4H_{10}$  (70:23:7) for fast neutron detection. The gas flow rate for all gas types was again kept constant at 3.0 L/hr throughout the measurement. The neutron test setup is shown in Fig. 5. The neutron source used in neutron

tests was a 300-mCi <sup>241</sup>Am/Be. The 10-cm lead bricks were used as gamma shields to ensure negligible contributions from gamma to neutron measurement.



**Fig. 5.** Neutron test setup consisting of a neutron source (<sup>241</sup>Am/Be), paraffin for neutron shielding, 10-cm lead bricks for gamma shielding, and a GEM detector.

## 2.2.1 Relative efficiency and relative gain tests

To measure relative efficiencies and relative gains for all three gas types, the supplied high voltages were varied from -3900 to -4400 V in 50-V increments. For each high voltage setting, 10 sets of one-hour-long tests were performed in order to find average signal count rates and signal amplitudes. The signal counts were measured using a counter/timer (Canberra Model 2071A) with a threshold of 0.1 A.U., while the signal amplitudes were measured using an average amplitude function available in Hantek DSO5202B oscilloscope. Proper background counts from cosmic radiation measured by the GEM detector without a neutron source presented were measured and subtracted from measured signal counts to ensure only neutron data was included in the calculations. Another interesting investigation would be to compare the efficiencies of neutron detection through nuclear reactions and elastic scattering. In order to compare the two methods, the GEM system was modified by following procedures: coating the

drift cathode with  $1-\mu m^{-10}B$ , inserting 5-cm HDPE sheets between lead bricks and the GEM detector to thermalize fast neutrons, and flowing the gas mixture of Ar/CO2 (70:30) to the detector at a constant flow rate of 3.0 L/hr. Five sets of 3-minute tests were performed to find average count rates.

# 2.2.2 Uniformity test

To investigate detection uniformity of the GEM detector for all three gas types, the supplied high voltage was kept constant at -4300 V. To allow only a small active area of the GEM detector to be exposed to fast neutrons, additional materials that completely shield neutrons from exposing to other areas were introduced to the setup. The materials used were 5-cm HDPE sheets, which acted as moderators, and 1-inch flexible neutron shield sheets supplied by Shieldwerx (Model SWX-238). The designed combination of HDPE and neutron shield sheets were placed between the lead bricks and the GEM detector. A <sup>3</sup>He neutron detector was used to ensure negligible counts of neutrons had reached the GEM detector when the added materials were in place. The combined materials were then cut to have a 2-cm-diameter hole located at the intended position of the active area. The setup of the shielding materials is shown in Fig. 6. Five different positions on the active area were selected for investigation as shown in Fig. 7 and detection counts for each position were measured and compared.

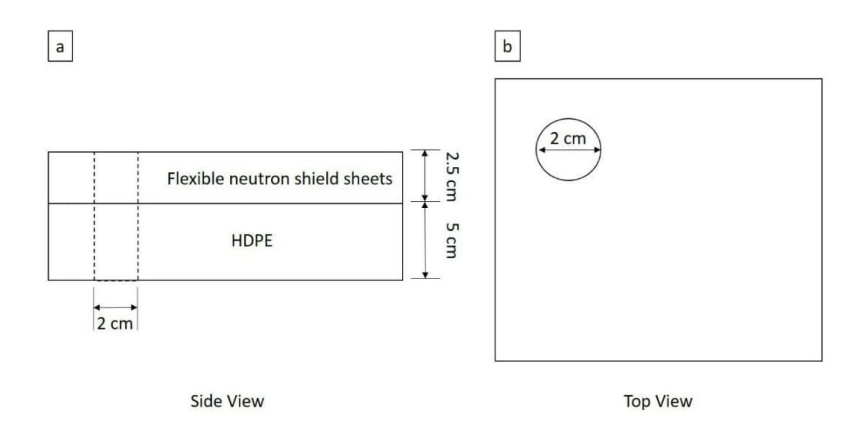


**Fig. 6.** Setup of neutron shielding for uniformity test, where (a) shows side view and (b) shows top view of the setup. A 2-cm hole was cut to let fast neutrons exposing to selected positions.

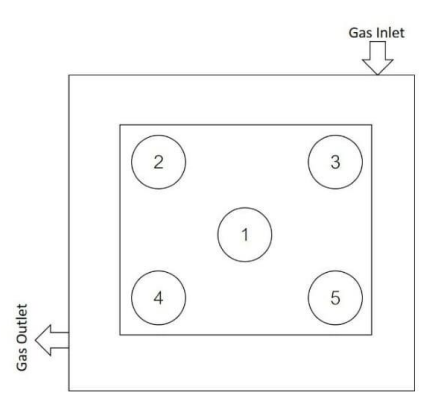


Fig. 7. Five different positions on the active area selected for uniformity test.

# 3. Results and discussion

# 3.1 Relative efficiency

To measure relative detection efficiencies for different values of high voltages supplied, three different gas types:  ${}^4\text{He/CO}_2$  (80:20 and 70:30) and  ${}^4\text{He/CO}_2/C_4H_{10}$  (70:23:7), were flowed

through the GEM detector. Average count rates were measured and calculated to compare relative efficiencies for each gas type.

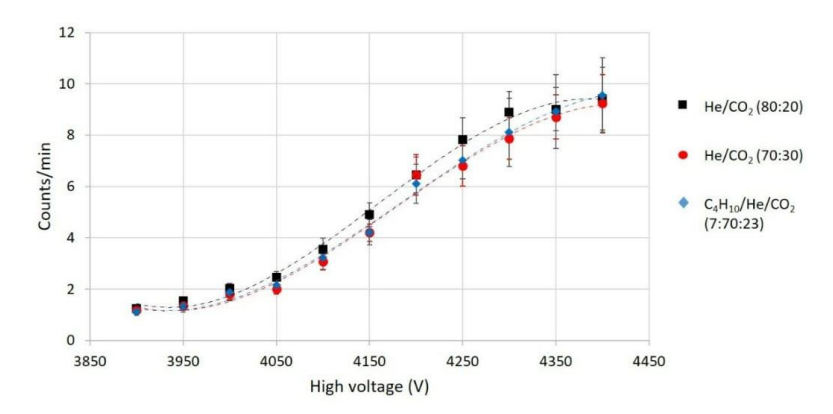


**Fig. 8.** The figure shows relative fast neutron detection count rates of the GEM detector flowed by gas mixtures of  ${}^{4}\text{He/CO}_{2}$  (80:20 and 70:30) and  ${}^{4}\text{He/CO}_{2}/C_{4}H_{10}$  (70:23:7).

As shown in Fig. 8, count rates increased as high voltages supplied increased and reached plateau region when the high voltage was  $\sim$  -4300 V, while flowing a gas mixture of  $^4\text{He/CO}_2$  (80:20) yielded slightly higher count rates amongst all three gas types. This behavior was due to the highest concentration of light nuclei, specifically  $^4\text{He}$ , in  $^4\text{He/CO}_2$  (80:20), which the energy transfer from incoming fast neutrons to recoil nuclei was larger as shown in Eq. 1. However, when considering stability of signals, it was found that the gas mixture of  $^4\text{He/CO}_2$ /C4H10 (70:23:7) gave more stable signals as less discharged frequencies and electrical noises were observed. The increase in signal stability from adding  $C_4H_{10}$  agreed with results reported in Bencivenni et al, 2003 and Alfonsi at al., 2004.

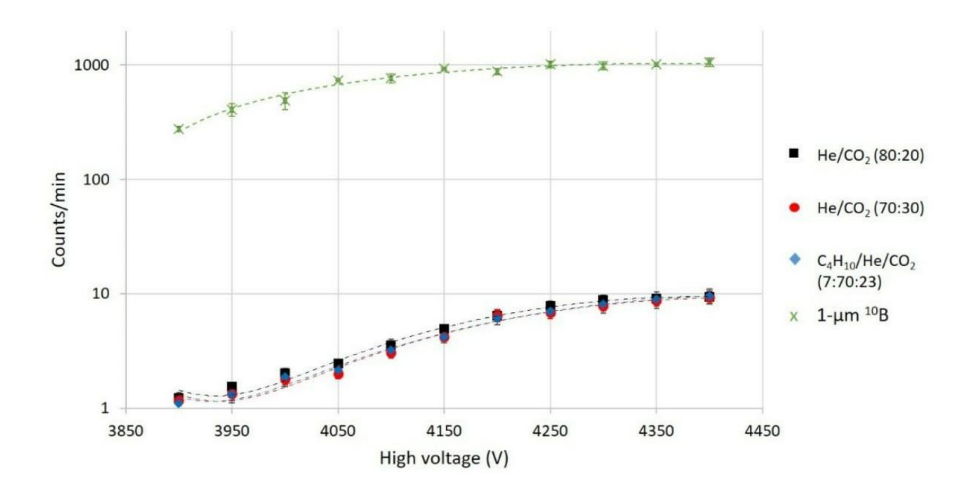


**Fig. 9.** Relative neutron detection count rates of the GEM detector flowed by (i)  $^4$ He/CO<sub>2</sub> (80:20), (ii)  $^4$ He/CO<sub>2</sub> (70:30), (iii)  $^4$ He/CO<sub>2</sub>/C<sub>4</sub>H<sub>10</sub> (70:23:7), and (iv) Ar/CO<sub>2</sub> with 1- $\mu$ m  $^{10}$ B-coated drift cathode.

For comparisons on detection efficiencies through nuclear reactions and elastic scattering, as shown in Fig. 9, count rates from the GEM detector flowed by Ar/CO<sub>2</sub> with 1- $\mu$ m 10 B-coated drift cathode were approximately 100 times larger than the standard GEM detector flowed by  $^4$ He/CO<sub>2</sub> (80:20 and 70:30) and  $^4$ He/CO<sub>2</sub>/C<sub>4</sub>H<sub>10</sub> (70:23:7). This result was expected as thermal neutrons are more likely to interact with  $^{10}$ B nuclei via nuclear reactions, which have high neutron absorption cross section.

#### 3.2 Relative Gains

To measure relative gains for different values of high voltages supplied, three different gas types:  ${}^{4}\text{He/CO}_{2}$  (80:20 and 70:30) and  ${}^{4}\text{He/CO}_{2}/C_{4}H_{10}$  (70:23:7), were flowed through the GEM detector. Average signal amplitudes were measured and calculated to compare relative gains for each gas type.

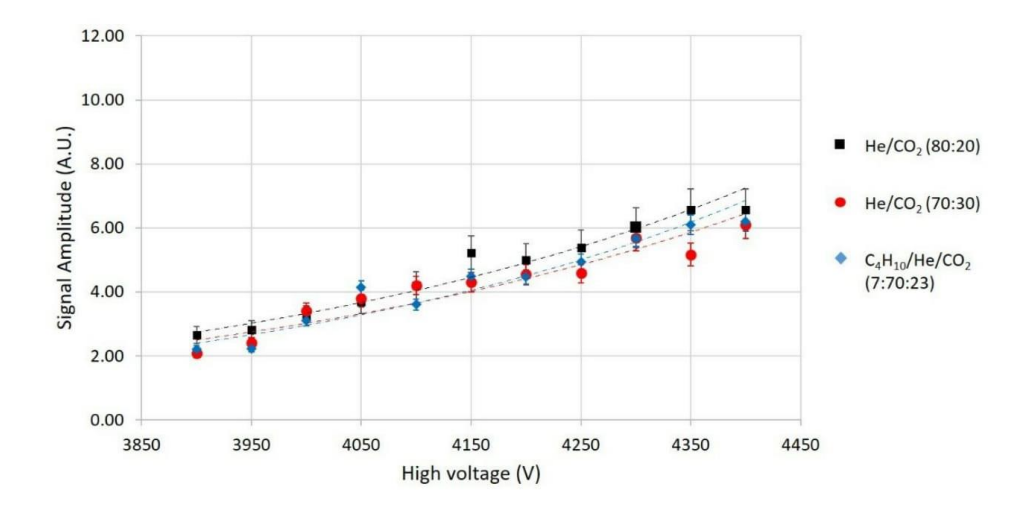


Fig. 10. Signal amplitudes of the GEM detector flowed by gas mixtures of  ${}^4\text{He/CO}_2$  (80:20 and 70:30) and  ${}^4\text{He/CO}_2/\text{C}_4\text{H}_{10}$  (70:23:7)

As shown in Fig. 10, gains, which are represented by signal amplitudes, increased as high voltages supplied increased, while flowing a gas mixture of  $^4\text{He/CO}_2$  (80:20) gave slightly higher gains amongst all three gas mixture types. This was because  $^4\text{He/CO}_2$  (80:20) had higher  $^4\text{He}$  concentrations, thus, an incoming fast neutron could scatter with  $^4\text{He}$  nuclei more frequently, creating larger groups of ionized electrons.

# 3.3 Uniformity

To measure detection uniformity of the GEM detector, five different positions on the 10 cm×10 cm active area were selected and neutron detection counts were measured.

**Table 1.** Normalized neutron count rates from five different positions on GEM's active area flowed by three different gas mixtures.

Position —		Gas Mixtures	
	<sup>4</sup> He/CO <sub>2</sub> (80:20)	<sup>4</sup> He/CO <sub>2</sub> (70:30)	<sup>4</sup> He/CO <sub>2</sub> /C <sub>4</sub> H <sub>10</sub> (70:23:7)
1	1.00	0.98	0.97
2	0.76	0.75	0.75
3	0.82	0.80	0.81

4	0.80	0.80	0.80
5	0.75	0.75	0.76

From Table 1, count rates from the center of the active area were approximately 20% higher than from other four positions closer to the edges of the detector. This was due to the fact that ionized electrons produced from elastic scattering near edges had possibilities to travel or drift out of the active area, making their signal amplitudes smaller than threshold and lowering their overall efficiencies. Another interesting result from the test was that the two positions at the gas inlet/outlet corners had  $\sim$ 5% higher in count rates than the other two corners. This might be due to gas pathways from gas inlet to gas outlet, which were non-uniformly distributed across the active area. The same behavior was also observed in Saenboonruang *et al.*, 2016 where gamma rays were used to measure uniformity of the detector.

#### 4. Conclusions

A GEM detector, which is typically used for ionizing particle detection, has potentials to be used as a neutron detection. In this research, a GEM detector was used to detect fast neutrons through elastic scattering between fast neutrons and light nuclei. Gas mixtures of <sup>4</sup>He/CO<sub>2</sub> (80:20 and 70:30) and <sup>4</sup>He/CO<sub>2</sub>/C<sub>4</sub>H<sub>10</sub> (70:23:7) were flowed through a GEM detector at a constant flow rate of 3.0 L/hr. Results showed that the detector was able to detect fast neutrons with different efficiencies and gains, where the gas mixture of <sup>4</sup>He/CO<sub>2</sub> (80:20) yielded highest values in both properties. However, when the results were compared with a setup where the GEM drift cathode was coated by a 1-µm 10 B to induced nuclear reactions, detection efficiencies through elastic scattering were approximately 100 times smaller. This was due to a much higher neutron cross section for 10B nuclei. In terms of detection uniformity of the detector, a position near the center of the active area had approximately 20% higher detection efficiencies than positions close to edges. At the same time, positions near gas inlet/outlet corners had approximately 5% higher detection efficiencies than the other two corner positions. These results had confirmed that, even though the detection efficiency through elastic scattering was less than those of detection through nuclear reactions, the GEM detector flowed by 4He-contained gas mixtures could detect fast neutrons with relatively simpler modifications to existing detectors.

## 5. Acknowledgments

This work was supported by The Thailand Research Fund (TRF) under Grant No. TRG5780292; Kasetsart University, and Faculty of Science under Grant No. RFG2-5. We would also like to acknowledge supports from Kasetsart University Research and Development Institute (KURDI), Department of Applied Radiation and Isotopes, Thailand Institute of Nuclear Technology (TINT), and the National Electronics and Computer Technology Center (NECTEC), Thailand.

#### References

- **Alfonsi, M. et al. (2004)** High-rate particle triggering with triple-GEM detector. Nucl. Instr. Meth. Phys. Res. A. **518**: 106-112.
- Anderson, H. et al. (2003) GEM detectors for X-ray astronomy. Nucl. Instr. Meth. Phys. Res. A. 513: 155-158.
- **Bayanov**, **B.F. et al. (1998)** Accelerator based neutron source for the neutron-capture and fast neutron therapy at hospital. Nucl. Instr. Meth. Phys. Res. A. **413**(2-3): 397-426.
- **Bencivenni, G. et al. (2003)** Advances ub triple-GEM detector operation for high-rate particle triggering. Nucl. Instr. Meth. Phys. Res. A. **513**: 264-268.
- Crane, T.W. & Baker, M.P. (1991) Neutron Detectors: Passive Nondestructive Assay of Nuclear Materials (Nuclear Regulatory Commission). Pp.379.
- Danielson, M., Fonte, P., Francke, T., Iacobaeus, C., Ostling, J. & Peskov, V. (2004) Novel gaseous detector for medical imaging. Nucl. Instr. Meth. Phys. Res. A. 518: 406-410.
- **Douglas, J.G., Koh, W., Austin-Seymore, M. & Laramore, G.E. (2003)** Treatment of salivary gland neoplasms with fast neutron radiotherapy. Arch. Otolaryngol. **129**(9): 944-948.
- **Eberhardt, J.E., Stevens, R.J., Sowerby, B.D. & Tickner, J.R. (2005)** Fast neutron radiography scanner for the detection of contraband in air cargo containers. Appl. Radiat. Isot. **63**: 179-188.

- Gnanvo, K., Liyanage, N., Nelyubin, V., Saenboonruang, K., Sacher, S. & Wojtsekhowski,
  B. (2015) Large size GEM for Super Bigbite Spectrometer (SBS) polarimeter for Hall A
  12 GeV program at JLab. Nucl. Instr. Meth. Phys. Res. A. 782: 77-86.
- Gozani, T. & Strellis, D. (2007) Advances in neutron based bulk explosive detection. Nucl. Instr. Meth. Phys. Res. B. 261: 311-315.
- Lacy, J. L., Athanasiades, A., Sun, L., Martin, C.S., Lyons, T.D., Foss, M.A. & Haygood, H.B. (2011) Boron-coated straws as a replacement for <sup>3</sup>He-based neutron detectors. Nucl. Instr. Meth. Phys. Res. A. 652: 359-363.
- Laramore, G.E., Krall, J. M., Griffin, T.W., Duncan, W., Richter, M.P., Saroja, K.R., Maor, M. H. & Davis, L.W. (1993) Neutron versus photon irradiation for unresectable salivary gland tumors: final report of an RTOG-MRC randomized clinical trial. Radiation Therapy Oncology Group. Medical Research Council. Int. J. Radiat. Oncol. 27(2):235-240.
- Miller, T.G. & Makky, W.H. (1993) Application of Fast Neutron Spectroscopy/Radiography (FNS/R) to Airport Security. Proc. SPIE. 1737: 184-196.
- Ohshita, H. et al. (2010) Development of a neutron detector with a GEM. Nucl. Instr. Meth. Phys. Res. A. 623: 126-128.
- Prasad, K. R., Dighe, P. M. & Alex, M. (2000) Boron-lined neutron detectors with gamma discrimination for reactor applications. Indian. J. Eng. Mater. S. 7: 21-24.
- **Saenboonruang, K. (2015)** Recent developments on GEM-based neutron detectors. J. Phys. Conf. Ser. **611**: 012016.
- **Saenboonruang, K., Kumpiranon, P., Kulasri, K. & Rittirong, A. (2016)** Effects of high gas flow rates on the standard 10 cm x 10 cm GEM prototype. Chiang Mai J. Sci. **43**(4): 875-882.
- Sauli, F. (1997) GEM: A new concept for electron amplification in gas detectors. Nucl. Instr. Meth. Phys. Res. A. 386: 531.

# 8. Output (Acknowledge the Thailand Research Fund)

## 8.1 International Journal Publication

- K. Saenboonruang\*, "Recent developments in GEM-based neutron detectors", Journal of Physics: Conference Series 611 (2015) 012016
- K. Saenboonruang\*, P. Kumphiranon, K. Kulasri, and A. Ritthitong, "Investigation on Properties of the 10 cm × 10 cm GEM Prototype"
   (Under review for publication on "Maejo International Journal of Science and Technology")
- K. Saenboonruang\*, P. Kumphiranon, J. Channuie, and T. Vilaithong, "Comparisons of GEM-Based Neutron Detectors with <sup>10</sup>B/<sup>nat</sup>B-coated Cathode and Ar/CO<sub>2</sub> (He/CO<sub>2</sub>) Gas Flow" (under review for publication on "Chiang Mai Journal of Science")
- K. Saenboonruang\*, P. Kumphiranon, K. Chirapatpimol, T. Vilaithong, "Comparison of a GEM-based Fast Neutron Detector Using <sup>4</sup>He/CO<sub>2</sub> and <sup>4</sup>He/CO<sub>2</sub>/C<sub>4</sub>H<sub>10</sub> Gas Mixtures" (under review for publication on "Kuwait Journal of Science")

# 8.2 Applications

- Teaching materials for classes:
  - "Selected Topics in Applied Radiation and Isotopes"
  - "Nuclear Facilities"
  - "Nuclear Sciences"
  - "Seminar"

# 8.3 International Conference

K. Saenboonruang\*, "Recent developments in GEM-based neutron detectors", International Nuclear Science and Technology Conference 2014 (INST2014), Bangkok, Thailand, 30-31 August, 2014.